



Ca' Foscari  
University  
of Venice

Master's Degree programme  
in Economics and Finance

Final Thesis

# Investing in Solar Energy under Price and Cost Uncertainty

**Supervisor**

Prof. Luca Di Corato

**Graduand**

Davide Righetto

Matriculation Number 857575

**Academic Year**

2020 / 2021



# Index

Abstract .....	1
I. Introduction.....	3
II. Theoretical Background .....	9
II.1 Stochastic Models .....	9
II.1.1 White Noise .....	9
II.1.2 Symmetric Random Walk (SRW) .....	10
II.1.3 Scaled Symmetric Random Walk.....	14
II.1.4 Brownian Motion.....	14
II.1.5 Geometric Brownian Motion.....	17
II.2 Augmented Dickey Fuller Test.....	19
III. Prices .....	21
III.1 Development of the European Electric Markets and the IPEX.....	21
III.2 Time series of the Energy Prices.....	24
III.3 Inflation Adjustment .....	26
III.4 Log Transformation .....	28
III.5 Deseasonalization.....	29
III.6 Independence and Normality.....	31
III.7 Non-stationarity .....	32
III.8 Parameters Estimation .....	34
III.9 Final Consumer Price.....	36
IV. Costs .....	39
IV.1 Measures of Cost.....	39
IV.2 Global Trend of PV solar energy costs.....	41
IV.3 Italy's PV solar energy costs data .....	43
IV.4 Learning Curve.....	45

IV.5	LCOE's values for the stochastic Grid Parity model .....	48
V.	Grid Parity.....	51
V.1	Standard Grid Parity .....	51
V.2	Dynamic Programming and Contingent Claim Approaches .....	52
V.2.1	The Approach applied to our model .....	60
V.3	Real Option Approach .....	64
VI.	Conclusions.....	70
	Appendix.....	72
A.	Proofs .....	72
A.1	Variance of the Random Walk .....	72
A.2	Derivation of the GBM solution formula .....	73
A.3	Expected Value of the GBM .....	75
A.4	Proof of the Martingale Property for the Symmetric Random Walk.....	76
A.5	Proof of the Martingale Property for the Brownian Motion Increments .....	76
B.	Prices .....	77
B.1	PUN Monthly Average Data .....	77
B.2	Inflation Rates in Italy.....	78
B.3	Augmented Dickey Fuller tables.....	78
B.4	ARERA End User Prices for Energy .....	79
C.	Grid Parity.....	80
C.1	Expected grid parity time .....	80
C.2	Partial Derivative of E(t) with respect to $\mu$ .....	82
	References.....	83

## Abstract

This thesis has the aim to evaluate the profitability of an investment in a photovoltaic system when considering uncertain energy prices and costs. We determine the optimal investment timing using a standard Grid Parity model and then compare it with the optimal timing determined using a stochastic Grid Parity model taking into account the presence of an option value to invest. This model required the calibration of two Geometric Brownian Motions (GBM) that have been used to express the future paths of prices and costs. The GBM's drift and volatility of the prices have been calibrated through an analysis of the trend and the volatility of the time series Prezzo Unico Nazionale, that is the price formed in the Italian Power Exchange (IPEX). On the other hand, the estimation of the parameters related to the costs of the PV plant has been performed applying the learning curve approach to the evolution of the PV sector and considering the stocks' volatility of the main companies producing PV modules. The two GBM processes calibrated in this way then have been included in the stochastic Grid Parity model with the aim to forecast the timing at which the investment in a PV plant becomes profitable, involving in the evaluation also the uncertainty surrounding the future paths of prices and costs. In the end of the thesis, we will show that the stochastic Grid Parity leads to considerable differences with respect to the standard version about the optimal time that a rational agent should choose to invest in the PV plant.



## I. Introduction

In the last decade, the potential of the photovoltaic (PV) energy production in Italy has undergone significant changes as shown by the variation of the total Installed Capacity (IC) over time.

Until 2007 the total Installed Capacity (IC) of the PV sector in Italy was relatively low since it was equal to only 87 MW. It started growing considerably only in 2008 when it reached 483 MW, that is, an increase equal to more than 450% with respect to the previous year<sup>1</sup>. The growth continued to be very high in the two following years (with an average increase around 170%) but the main relevant year for the sector was 2011 with the addition of 9000 MW of installed PV capacity reaching a total IC equal to 12780 MW. Thanks to this rapid development, Italy has become one of the leaders in the PV energy production among the developed countries with the second largest PV installed capacity in Europe after Germany<sup>2</sup>. In 2012 the growth started to slow down but it was still relatively high with an increase rate equal to 30% and a total IC equal to 16480 MW. In Figure 1, we can see that the growth rate of the total capacity has dropped dramatically after 2013. In the period between 2014 and 2018 the additional capacity installed was about 400 MW per year (corresponding to a steady annual increase rate around 2%), very far from the growth experienced in the previous years. In 2019 the additional capacity was higher with respect to 2018 and equal to 757 MW, determining a small increase in the yearly growth rate (3.8%) which led to a total IC of 20860 MW. The peculiar growth path of the PV sector in Italy is directly related to the public incentives aimed to support the investment in this type of source of energy.

In particular, the feed-in-tariff denominated *Conto Energia*, articulated in 5 different schemes between 2005 and 2013, had a relevant impact in the expansion of the sector through a mechanism of payments financed by the Government on the basis of the cost of the PV technology.

---

<sup>1</sup> All the data about the Italian PV installed capacity in this Section are available on the website of Gestore dei Servizi Energetici (GSE). The data presented here are the most updated and may show small differences with data shown in past reports by GSE

<sup>2</sup> See "Rapporto Statistico 2011", GSE, p. 38

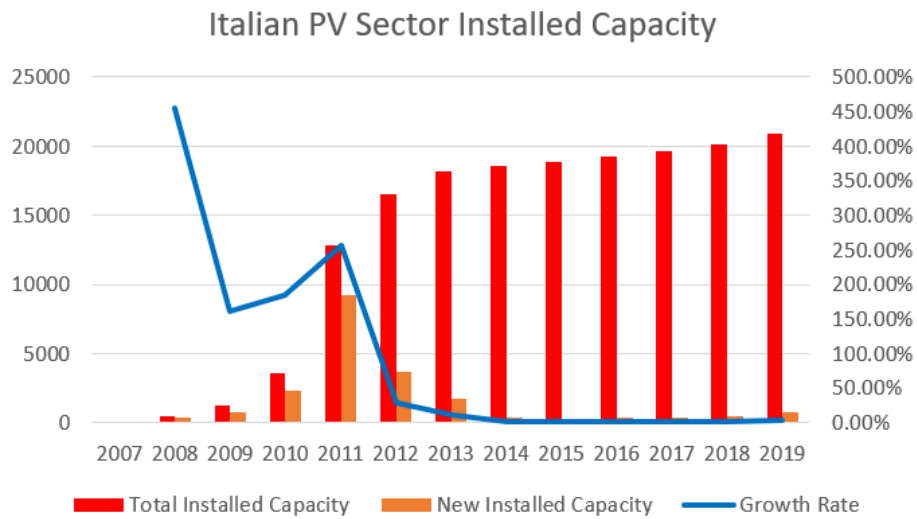


Figure 1: Italian PV Sector Installed Capacity (elaboration on GSE data)

The end of *Conto Energia* in 2013 had a negative effect on the growth rates of the installed capacity in the following years showing the dependence of the expansion of the PV market on public incentives<sup>3</sup>.

What have been said until now may call for an evaluation of the actual profitability of the investment in a PV plant.

One of the most used methodologies applied in the evaluation of PV investment is the Grid Parity. The Grid Parity represents a sort of break-even point in that it is defined as the point in time where the price of energy purchased on the market equals the unit cost of energy produced through a PV plant. The starting scenario is usually characterized by a unit cost of energy higher than the price of energy and by the following future prospects: (i) a price increase against a cost reduction, (ii) price increasing faster than costs or (iii) price diminishing slower than costs. Given the starting scenario, in all these three situations at a certain time point in the future price is expected to equal and then exceed the cost. By comparing the price that a consumer pays for one unit of energy purchased from a provider and the cost of producing one unit of energy through its own plant, the Grid Parity determines which one it's the cheapest way for obtaining that unit. Using the Grid Parity, it is possible to estimate the

<sup>3</sup> The relationship between the end of *Conto Energia* and the Total Installed Capacity growth rates is recognized also in "Rapporto Statistico GSE 2019" p. 44

optimal time for investing in a PV plant in the light of the evolution of energy prices and project costs.

As shown by Biondi and Moretto (2013), the limit of the standard approach is that it is not able to include in the analysis two important factors characterising the investment in a PV plant, i.e., (i) the high initial investment cost which is largely irreversible and (ii) the uncertainty surrounding the future paths of both electricity prices and costs related to the PV plant's installation. The irreversibility of the investment is important because, according to the standard Grid Parity, once that the price of energy is higher than the costs of the PV technology it is already optimal to invest in the plant. Therefore, the model does not consider that if a subsequent fall in price or rise in cost should occur, pushing again costs above price, the investment would no more be profitable. This makes the second shortcoming relevant since a correct interpretation of the uncertainty characterising the variables considered gives the possibility to include the evaluation of this risk in the investment decision, presumably requiring a deeper "in-the-money" situation (using a parallelism with option theory) with a higher margin between price and cost needed to trigger the decision, which implies a delay in the timing of the investment.

To overcome these shortcomings, in this thesis we use the "stochastic Grid Parity" proposed by Biondi and Moretto (2013). This model, developed under a Real Options approach<sup>4</sup>, allows including in the evaluation the cost-opportunity of investing at a specific time point giving up the information about the future realization of prices and costs which can potentially affect the expected payoff of the investment. By so doing, the Grid Parity is determined taking into account the value of the option to defer the investment.

The application of the model in this thesis required the calibration of the two Geometric Brownian Motions assumed in order to describe the stochastic evolution of prices and costs.

The parameters related to prices, namely trend and volatility, have been estimated considering the time series of the Prezzo Unico Nazionale (PUN) which is the price that is formed in the Italian Power Exchange (IPEX) taken as a reference for the energy prices

---

<sup>4</sup> See Dixit and Pindyck (1994)

in Italy. This time series has been subjected to a step-by-step data treatment to correctly estimate the necessary parameters: first of all, we reduced the observations keeping the prices in the daily interval between 8:00 and 19:00 (that is approximately the time interval with an adequate solar exposition for a PV plant), then the series has been corrected removing the effect of the inflation with the actualization of the prices to December 2019 and after that the data has been expressed in logarithmic form. At this point we performed the deseasonalization procedure necessary to remove eventual seasonal autocorrelation that could characterize prices related to the consumption of energy.

The logarithmic returns of the time series built in this way were tested for independence with the correlogram resulting in the absence of autocorrelation for several lags (also because of the deseasonalization treatment) and they were also tested for normality with the QQ-Plot which indicated an empirical distribution close to the normal one. These two results suggested the plausibility for the PUN series to be modelled as a Geometric Brownian Motion (GBM). Furthermore, we performed the Augmented Dickey Fuller test on the logarithmic returns to test the stationarity of the time series and the test did not reject the null hypothesis of non-stationarity which is an indication for the plausibility of the assumed GBM model.

At the end of the treatment of the data just described, it has been possible to estimate the historical trend and volatility exploiting the properties of the logarithmic returns related to the two parameters of the GBM.

On the other side, we performed a parallel analysis on the costs related to a PV plant in order to estimate the parameters of trend and volatility necessary for the stochastic Grid Parity model. We considered as a reference for the unitary cost of the investment in a PV plant the Levelized Cost of Energy which is an indicator that expresses in a single number all the different expenses that this type of investment involves all along its economic lifetime, starting from installation costs to the maintenance ones, actualizing them at a specific moment and dividing for the expected output produced by the plant. To estimate the trend determining the evolution in time of this indicator, we followed the Learning Curve approach. The idea behind this approach is that the cost related to the production of something in a given market is conditioned by the technological progress reached in that sector and the experience that the agents in that market have

developed as it becomes more mature: in a relatively young sector like the photovoltaic one we can expect to have still a considerable margin for cost reduction whose trend can be estimated with the Learning Curve approach.

The other parameter necessary for our model, i.e., the volatility characterising the future evolution of the cost, was more complex to estimate directly because of the various different expenses composing the total cost of the plant. To overcome this difficulty, we took as a proxy for the volatility of the cost of the PV plant the average of the volatilities of the market shares of the biggest companies producing PV modules (data that are readily available) considering that the cost of the modules is the most important factor affecting the overall cost of the PV plant.

Finally, using the estimated parameters, we compared the results obtained using a standard Grid Parity model with those obtained using the stochastic Grid Parity. We show that using the latter approach leads to a significant postponement of the optimal timing choice as a consequence of the inclusion in the investment evaluation of the option value associated with the PV investment project.

The thesis includes 6 chapters. Once introduced the problem in Chapter 1, in Chapter 2 we briefly present the theory behind a Geometric Brownian Motion (GBM), that is, the process that we will use to model the random evolution of both prices and costs over time. Chapter 3 presents the development of the Italian energy market from which the data about the prices of electricity have been collected. This chapter contains the analysis that has been performed on the time series of the prices and the estimation of the relevant parameters characterizing its dynamic. In Chapter 4 we discuss the recent trend of the Levelized Cost of Energy (LCOE) for the PV sector. We then determine the parameters characterizing the dynamic of the LCOE. In Chapter 5 we present the models used in our numerical exercise, that is, i) the standard Grid Parity model and ii) the stochastic Grid Parity model. We calibrate both models using the parameters estimated in the previous Chapters and calculate the expected investment time considering 2019 as starting point. Chapter 6 concludes. At the end of the thesis there is an Appendix where we provide tables and figure concerning the data analysis and the proofs related to the models presented.



## II. Theoretical Background

### II.1 Stochastic Models

A fundamental assumption in this thesis is that electricity prices in the Italian market and costs related to a PV plant evolve over time following a Geometric Brownian Motion. In the next Sections, we present the main properties of the GBM starting from the simpler processes needed for its comprehension, i.e., White Noise, Random Walk and Brownian Motion.

A Brownian Motion is a stochastic process and as such it satisfies the general propriety of any stochastic process, that is:

*“A stochastic process is a collection of random variables that takes values in a set  $S$ , the state space, and that is indexed by another set  $T$ , the index set<sup>5</sup>”.*

This simply means that the random variables of a stochastic process must be ordered in time.

The Brownian Motion can be conceptualized starting from the *Symmetric Random Walk (SRW)*<sup>6</sup>, a process based on its closest past realization and a White Noise.

#### II.1.1 White Noise

A White Noise is the simplest example of a stationary stochastic process. A time series  $a_t$  is a White Noise if the sequence is composed by independent and identically distributed random variables with constant mean, constant variance and correlation equal to 0 for all lags:

$$a_t \sim WN(\mu, \sigma^2) \tag{1}$$

where<sup>7</sup>

- $E(a_t) = \mu$  for any time period  $t$

---

<sup>5</sup> See Olofsson and Andersson (2011), p. 455

<sup>6</sup> See Shreve (2004) p. 83-84

<sup>7</sup> See Ruppert (2011), p.205

- $Var(A_t) = \sigma^2$  (a constant) for any  $t$
- $Corr(A_t, A_{t+j}) = 0$  for any  $j \neq 0$

Note that since mean and variance are constant over time, a White Noise is a stationary process.

Note that as  $Corr(A_t, A_{t+j}) = 0$ , in order to determine if a time series could be modelled as a white noise, the coefficients of its Auto Correlation Function (ACF) must be not significantly different from 0.

A relevant property of the White Noise comes from the absence of autocorrelation. Indeed, it is possible to prove that the past realizations of the process have no impact on the capacity to predict the future realizations of the process itself<sup>8</sup>:

$$E(A_{t+j} | A_1, \dots, A_t) = \mu \quad \text{for all } j \geq 1 \quad (2)$$

One of the most used versions of White Noise is the Gaussian White Noise which is often included into more complex models: its particularity arises from the fact that the random variables of this process are *normally* distributed with mean 0 and variance  $\sigma^2$ .

### 11.1.2 Symmetric Random Walk (SRW)

The previous properties of a White Noise are essential for the following considerations about the Random Walk.

A Random Walk is a process  $y_t$  which takes the following form:

$$y_t = y_{t-1} + a_t, \text{ where } a_t \sim WN(0, \sigma^2) \quad (3)$$

with  $y_0 \in \mathbb{R}$  as starting value and where  $a_t$  is a white noise process.<sup>9</sup>

Being the starting value  $y_0$  known, we can say that at each point in time  $t$ ,  $y_t$  is equal to  $y_0$  plus the sum of all the past realizations of  $a_t$ :

$$y_t = y_0 + \sum_{i=1}^t a_i \quad (4)$$

---

<sup>8</sup> See Tsay (2013), p. 86-87

<sup>9</sup> See Tsay (2013), p. 87

The expected value of the process is simply coincident with its known starting point.

$$E(y_t) = E\left(y_0 + \sum_{i=1}^t a_i\right) = y_0 \quad (5)$$

A Random Walk is a non-stationary process since its variance increases over time<sup>10</sup>. Note in fact that:

$$Var(y_t) = E(\sum \sum a_i a_j) = t\sigma^2 \quad (6)$$

The Autocovariance of a Random Walk is also dependent on the time lag:

$$\gamma_{s,t} = \begin{cases} \sigma^2 t & t = s \\ \sigma^2 \min(s, t) & t \neq s \end{cases}$$

From the discussion above it is important to underline that the Random Walk comprehends White Noise as one of its elements but it does not maintain the property of a stationary time series. In a Random Walk it is straightforward to recover the stationarity through an operation of first difference that implies the isolation of the White Noise:

$$\Delta y_t = y_t - y_{t-1} = a_t \quad (7)$$

The Symmetric Random Walk SRW is a particular type of Random Walk which can be distinguished from the general process mainly because of the characteristics of its probability distribution.

The construction of a SRW is ideally based on the formalization of a time series composed by random variables characterized by two possible outcomes, A and B, each with probability  $\frac{1}{2}$ .

---

<sup>10</sup> See Appendix A.1 for a proof.

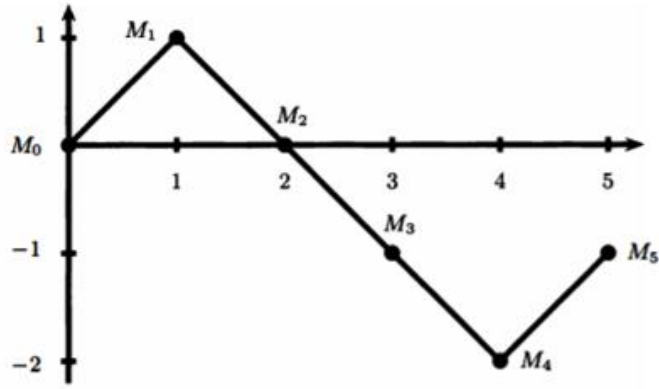


Figure 2: Steps of a Symmetric Random Walk (Shreve 2004)

We define  $\omega_n$  the outcome of the n-th trial and let:

$$X_j = \begin{cases} 1 & \text{if } \omega_j = A \\ -1 & \text{if } \omega_j = B \end{cases} \quad (8)$$

Finally, we define  $M_0 = 0$  and:

$$M_k = \sum_{j=1}^k X_j \quad k = 1, 2, \dots \quad (9)$$

The process  $M_k$  is a *symmetric random walk*, at each step this process has two possibilities: either going up by one unit or going down by one unit.

Looking forward to what we are going to discuss later about the Brownian Motion, it is important to go in depth about three aspects of the SRW: its increments, its Martingale Property and its Quadratic Variation.

The increments of a random walk are *independent*. For integer values

$$0 = k_0 < k_1 < \dots < k_m$$

the random variables

$$M_{k_1} = (M_{k_1} - M_{k_0}), (M_{k_2} - M_{k_1}), \dots, (M_{k_m} - M_{k_{m-1}})$$

are expected to be independent and the *increment* can be defined as follows:

$$\text{increment: } M_{k_{i+1}} - M_{k_i} = \sum_{j=k_i+1}^{k_{i+1}} X_j \quad (10)$$

The increment measures the change of the position of the random walk, as graphically represented in Figure 2, between time  $k_i$  and  $k_{i+1}$ . If increments of non-overlapping periods are considered, independence still holds because the events occurring at each period are, by assumption, independent.

The increments have variance equal to  $k_{i+1} - k_i$  as we can see in Eq. 13:

$$\text{Var}(X_j) = \text{E}(X_j^2) = 1 \quad (11)$$

$$\text{Cov}(X_j, X_i) = 0 \quad j \neq i \quad (12)$$

$$\text{Var}(M_{k_{i+1}} - M_{k_i}) = \sum_{j=k_i+1}^{k_{i+1}} \text{Var}(X_j) = \sum_{j=k_i+1}^{k_{i+1}} 1 = k_{i+1} - k_i \quad (13)$$

Knowing that the variance of the SRW increases by 1 for each time  $t$ , the variance of the increment over an interval from  $k$  to  $l$  is  $l-k$ .

After that, it is possible to demonstrate that the SRW is a martingale<sup>11</sup>.

The quadratic variation of the SRW is defined as:

$$[M, M]_k = \sum_{j=1}^k (M_j - M_{j-1})^2 = k \quad (14)$$

In the case of SRW, the quadratic variation takes the same value of the variance but its calculation is different: if the random variables were not symmetric with different probabilities for the upward and downward movements, the variance would be affected by this fact. Furthermore, while the variance is a theoretical concept, the quadratic variation is calculated considering the actual path that the process has taken.

---

<sup>11</sup> See Appendix A for the proof of the Martingale Property for the SRW

### II.1.3 Scaled Symmetric Random Walk

In order to recreate the instantaneous change of the Brownian Motion, the Symmetric Random Walk is scaled infinitely. Both time and the size of the movement are subduced to a scale factor.

The scaled symmetric random walk is written as:

$$W^{(n)}(t) = \frac{1}{\sqrt{n}} M_{nt} \quad (15)$$

with  $nt$  integer. In the points where  $nt$  is not an integer,  $W^{(n)}(t)$  is defined through the linear interpolation of the two closest points:

$$W^{(n)}(t) = \begin{cases} \frac{1}{\sqrt{n}} M_{nt} & \text{when } t = \frac{m}{n} \in N \\ \text{interpolation} & t \in \left(\frac{m}{n}, \frac{m+1}{n}\right) \end{cases} \quad (16)$$

### II.1.4 Brownian Motion

From Eq. 16 it is possible to obtain the Brownian Motion by taking the limit  $n \rightarrow \infty$ .

With  $t > 0$ , as  $n \rightarrow \infty$ , the distribution of the scaled random walk  $W^{(n)}(t)$  evaluated at time  $t$  converges to the normal distribution with mean zero and variance  $t$  because of the Central Limit Theorem.

The Central Limit Theorem<sup>12</sup> states that: let  $X_1, \dots, X_n, \dots$  be independent, identically distributed, real valued random variables with

$$E(X_i) = m \quad V(X_i) = \sigma^2 > 0$$

for  $i = 1, \dots$  set

$$S_n := X_1 + \dots + X_n$$

---

<sup>12</sup> See Evans (2014), p. 26

Then for all  $-\infty < a < b < +\infty$

$$\lim_{n \rightarrow \infty} P\left(a \leq \frac{S_n - nm}{\sqrt{n}\sigma} \leq b\right) = \frac{1}{\sqrt{2\pi} \int_a^b e^{-\frac{x^2}{2}} dx} \quad (17)$$

Finally, we can define the Brownian Motion using the limit of the Scaled SRW:

$$\underline{W}(t) = d - \lim_{n \rightarrow +\infty} W^{(n)}(t) \quad (18)$$

where “d” underlines the fact that this is a limit in distribution because the distribution of the scaled random walk  $W^{(n)}$  converges to the distribution of the process  $W(t)$ .

Considering a probability space with sample space  $\Omega$ , event space  $\mathbb{F}$  and probability function  $\mathbb{P}$ , we address a continuous function  $W(t)$  in  $t \geq 0$  for  $\omega \in \Omega$  that takes value 0 in time 0 ( $W(0) = 0$ ). This function is a Brownian Motion if for  $0 = t_0 < t_1 < \dots < t_m$  the increments:

$$W(t_1) - W(t_0), W(t_2) - W(t_1), \dots, W(t_m) - W(t_{m-1})$$

are independent and each of them has a normal distribution with zero mean and variance dependent only on the time lag:

$$E[W(t_{i+1}) - W(t_i)] = 0 \quad (19)$$

$$Var[W(t_{i+1}) - W(t_i)] = t_{i+1} - t_i \quad (20)$$

For considerations similar to those of the symmetric random walk, we can also state that the Brownian motion is a martingale<sup>13</sup>.

In the case of a martingale the information about the past realization can be ignored until the closest one in time to the one we want to predict. This means that any information concerning the past is fully embodied in the last observation.

---

<sup>13</sup> See Appendix A for a sketch of the proof of the Martingale property for the Brownian Motion increments.

In general terms the quadratic variation of a function  $f(t)$  defined for  $0 \leq t \leq T$  up to time  $T$  is defined:

$$[f, f](T) = \lim_{|\Pi| \rightarrow 0} \sum_{j=0}^{n-1} [f(t_{j+1}) - f(t_j)]^2 \quad (21)$$

As for the martingale property, the quadratic variation of the Brownian motion presents similar results to those of the Symmetric Random Walk even if the path to arrive to them is different because BM does not present natural step size as in the case of SRW. Brownian Motion' quadratic variation increases by 1 per unit of time, fixing  $\Pi = \{t_0, t_1, \dots, t_n\}$  as a partition of  $[0, T]$  (meaning that  $0 = t_0 < t_1 < \dots < t_n = T$ ) we have:

$$\lim_{|\Pi| \rightarrow 0} \sum_{j=0}^{n-1} (W(t_{j+1}) - W(t_j))^2 = T \quad (22)$$

It is worth stressing that  $[W, W](T) = T$  with probability tending to 1. This implies that there exist paths of the Brownian motion where the quadratic variation is not equal to  $t$  but their probability to occur is equal to 0.

The vast majority of functions have continuous derivatives, therefore, they are characterised by quadratic variation equal to 0. Brownian motion is non differentiable w.r.t to time which makes it not subjected to ordinary calculus that does not deal with quadratic variation. On the other hand, stochastic calculus considers also the quadratic variation as can be seen in the expression of the Ito-Doeblin Formula (which contains an extra term coming from the nonzero quadratic variation of the Brownian Motion) that is necessary for the mathematical derivation of the solution formula of the Geometric Brownian Motion that is presented later in the text.

### II.1.5 Geometric Brownian Motion

A Geometric Brownian Motion (GBM)<sup>14</sup> can be illustrated through the following stochastic differential equation (SDE):

$$\begin{cases} dX(t) = \alpha X(t)dt + \sigma X(t)dW(t) & t \geq 0 \\ X(0) = x_0 \end{cases} \quad (23)$$

$$\mu(t, X) = \alpha X \quad \text{drift}$$

$$\sigma(t, X) = \sigma X \quad \text{diffusion}$$

Note that that if the diffusion term is equal to 0, Equation 23 becomes an ordinary differential equation. Therefore, the diffusion term is the one which makes the GBM stochastic.

In general, a stochastic process P(t) is a diffusion if its local dynamics is representable with a SDE of this type:

$$X(t + \Delta t) - X(t) = \mu(t, X(t))\Delta t + \sigma(t, X(t))Z(t) \quad (24)$$

where Z(t) is a random variable with a given distribution acting as disturbance term, not affected by the information until time t while  $\mu$  and  $\sigma$  are deterministic functions.

The solution of Equation 23 requires the use of Ito's stochastic calculus. This is because, as well known, a Brownian motion is nowhere differentiable according to ordinary calculus.

An Ito Process is a stochastic process that has the integral form:

$$I(t) = I(0) + \int_0^t \Delta(u)dW(u) + \int_0^t \Theta(u)du \quad (25)$$

$W(t) \sim \text{Brownian motion}$

$X(0)$  constant

$\Delta(u), \Theta(u)$  adapted stochastic processes

---

<sup>14</sup> The Geometric Brownian Motion is a widely used process in Finance. See Le Gall (2016)

or the equivalent differential form

$$\begin{cases} dX(t) = \Delta(t)dW(t) + \Theta(t)dt & t \geq 0 \\ X(0) = x_0 \end{cases} \quad (26)$$

From this definition we can see that the Geometric Brownian Motion is an Ito Process and consequently we can use the rules of differentiation for this class of processes, in our case the Ito-Doebelin formula. The Ito-Doebelin formula comes from unified considerations about the implications of the non-zero quadratic variations of the Brownian motion  $BM[W, W](t) = t$  and the second order Taylor expansion.

On the basis of the considerations above, it is now possible to derive the solution<sup>15</sup> formula of the GBM:

$$X(t) = x_0 e^{\left(\alpha - \frac{\sigma^2}{2}\right)t + \sigma W(t)} \quad (27)$$

Once found the solution, it is also possible to express the expected value<sup>16</sup> of the GBM:

$$E(X(t)) = x_0 e^{\left(\alpha - \frac{\sigma^2}{2}\right)t} \cdot e^{\frac{\sigma^2}{2}t} = x_0 e^{\alpha t} \quad (28)$$

---

<sup>15</sup> The complete derivation is presented in Appendix A.2

<sup>16</sup> Proof in Appendix A.3

## II.2 Augmented Dickey Fuller Test<sup>17</sup>

This test will be used in Chapter 3 in order to assess the hypothesis of stationarity of the time series of the electricity prices.

The Augmented Dickey Fuller (ADF) Test is one of the most common tests together with Phillips-Perron test and KPSS test which are used to check the stationarity of a time series.

We start with a process similar to an Auto Regressive of order 1:

$$Y_t = \alpha Y_{t-1} + X_t \quad \text{for } t = 1, 2 \dots \quad (29)$$

where  $X_t$  is a stationary process.

We know that at these conditions  $Y_t$  is stationary if  $|\alpha|$  is strictly minor than one and it is nonstationary if it is equal to 1.

For this reason, we set  $\alpha = 1$  as the null hypothesis.

$X_t$  is supposed to be an Auto Regressive of order  $k$  of the type:

$$X_t = \phi_1 X_{t-1} + \dots + \phi_k X_{t-k} + e_t \quad (30)$$

$Y_t$  can be rewritten as follows:

$$\begin{aligned} Y_t - Y_{t-1} &= \alpha Y_{t-1} + X_t - Y_{t-1} = (\alpha - 1)Y_{t-1} + \phi_1 X_{t-1} + \dots + \phi_k X_{t-k} + e_t \\ &= \delta Y_{t-1} + \phi_1 X_{t-1} + \dots + \phi_k X_{t-k} + e_t \end{aligned} \quad (31)$$

In the equation above we can see that  $\alpha - 1$  has been replaced with  $\delta$ , which means that  $\alpha - 1 = \delta$ . Now because the null hypothesis provides  $\alpha = 1 \rightarrow \delta = 0$ , it follows that  $X_t = Y_t - Y_{t-1} \rightarrow X_{t-1} = Y_{t-1} - Y_{t-2}$  and so:

$$Y_t - Y_{t-1} = \delta Y_{t-1} + \phi(Y_{t-1} - Y_{t-2}) + \dots + \phi_k(Y_{t-k} - Y_{t-k-1}) + e_t \quad (32)$$

---

<sup>17</sup> See Cryer and Chan (2008) p. 219 and Tsay (2013) p. 91-96.

The test is performed through the regression of the observations in first difference<sup>18</sup> ( $Y_t - Y_{t-1}$ ) against the data itself non-differenced at time t-1 ( $Y_{t-1}$ ) and the  $k$  lags before in first difference. From this regression it is possible to estimate the  $\delta$  coefficient.

If  $\delta$  results significantly different from 0 (which means  $\alpha \neq 1$ ), the null hypothesis of non-stationarity can be rejected. This can be recognized through the test statistics of the coefficient estimated with the least squares' procedure.

The appropriate critical values for the different levels of significance are particular because the ADF test statistics is not distributed according to a  $t$ -distribution under the null hypothesis. The values to which the distribution of this statistic tends have been estimated by Fuller and must be used through the specific tables in order to verify whether the null hypothesis should be rejected or not.

The Augmented Dickey-Fuller test can be expressed in three different versions, according to three models that take into account the possibility to have a trend or a constant shift in the process. The decision about which of these tests is the more adapt for the time series analysed has an influence on the relative critical values. Model 1 can be considered the classical Augmented Dickey Fuller test, model 2 corrects the standard equation for the existence of a constant and model 3 introduces terms that embody the possibility that the series is not stationary around a fixed mean but it is stationary around a trend.

---

<sup>18</sup> That is,  $\Delta y_t = y_t - y_{t-1}$

### III. Prices

This chapter contains the presentation of the time series of the energy prices that has been used for the calibration of the parameters of the Geometric Brownian Motion. We start presenting the source of the data (the Italian electric exchange) with its legal framework and then we go through the various steps of the treatment of the time series needed for the parameters' estimation.

#### III.1 Development of the European Electric Markets and the IPEX

The development of the Italian Power Exchange (IPEX) is strictly related to the evolution of the different electric markets in the European Union, as we will see in this section.

The legal framework of the IPEX is based on several normative references, in particular:

- Law n. 481 of 14/11/1995 establishing the Authority for Electric Energy and Gas (Autorità per l'Energia Elettrica e il Gas, AEEG);
- EU Directive 96/92/CE establishing communitarian rules for the internal electric market;
- Legislative Decree n. 79/99 implementing the EU Directive in the national body of law and entrusting "Gestore del Mercato (GME)" for the regulation of the Italian electric exchange;
- EU Directive 2003/54/CE<sup>3</sup> repealing the previous Directive and implementing new norms for the generation and distribution of energy. This Directive defines the rules for the access to the market and the procedures that need to be applied in the public notices through which the market participants to the market are selected. The obligations to which the entities involved in the construction of new generating capacity must comply with are the following<sup>19</sup>:
  - the safety and security of the electricity system, installations and associated equipment;
  - protection of public health and safety;
  - protection of the environment;

---

<sup>19</sup> These are taken directly from the text of the EU Directive: <https://eur-lex.europa.eu/legal-content/EN/TXT/?uri=CELEX%3A32003L0054&qid=1620843123560>

- land use and siting;
  - use of public ground;
  - energy efficiency;
  - the nature of the primary sources;
  - applicant specific characteristics particular to the applicant, such as technical, economic and financial capabilities.
- Regulation 1228/2003 of the European Parliament and Council regulating the exchange of energy across the national borders;
  - Technical Guidelines regulating the Energy Market (“Testo Integrato della Disciplina del mercato elettrico”) which contain the standards to be applied and the procedures implementing the Decree 16/3/1999 n.79;
  - Law n. 239/2004 for the Rearrangement of the Energy Sector establishing the general objectives of the national energy policies.

The development of the Italian Energy Market was a direct consequence of the impulse given by the European Union in the form of the Directive 96/92/CE aiming at the harmonization of the European energy markets on a communitarian level. The transposition of the Directive by each member State led to the design of different platforms for the exchange of energy.

The first structured European electric market was the UK Pool activated in 1990. In 2001, this market was then replaced by the New Electricity Trading Arrangements (NETA) which was characterised by a model of decentralized bilateral exchanges.

The Nord Pool represents instead the first energy market working on a regional level. It was institutionalised in Norway in 1993 and since then it became the promotor of a process that resulted in the involvement of Sweden in 1996, Finland in 1998 and Denmark in 2000, thus being able to bring together all the energy exchanges in Scandinavia. In Spain, the energy market was activated in 1999 and was named Operador del Mercado Electrico (OMEL), while in the Netherlands, in the same year, a platform for the exchange of energy named Amsterdam Power Exchange (APX) was activated. In 2000, Germany introduced at the same time two energy exchanges: the first one in Frankfurt based on continuous bilateral trading and the second located in Leipzig based on an auction system. In 2002, the two systems merged into the European

Energy Exchange (EEX) based in Leipzig. In 2001, France activated its electric market named Powernext which was based on an auction mechanism. Finally, in 2002, Austria initiated the Energy Exchange Austria (EXAA) located in Graz.

The Italian Power Exchange (IPEX) was activated through the legislative decree 79/99 (d. lgs. n. 79/99)<sup>20</sup>. In accordance with the Directive (96/92/CE), the IPEX has developed following the prescriptions characterising all the markets in the European context<sup>21</sup>.

The IPEX has been active since 31<sup>st</sup> March 2004 under the control of the “Gestore dei Mercati Energetici S.p.A.” (GME) that is an entity instituted ad-hoc, by the same Decree 79/99, which acts as central counterpart in the transactions registered on the exchange<sup>22</sup>.

GME is totally owned by Gestore dei Servizi Elettrici S.p.A. (GSE) which is participated by the Italian Ministry of Economics and Finance that owns 100% of its shares<sup>23</sup>.

The GSE has also an exclusive and total participation in Acquirente Unico S.p.A. (AU) whose aim is to arrange supply contracts in order to guarantee availability of the productive capacity and the dispatchment of energy in condition of continuity and efficiency.

The electric exchange is not only a digital market but also a physical market where the frame for the injection and extraction of energy in the grid is defined. Hence, the exchange becomes a fundamental tool for developing a competitive market providing the context needed to have efficient equilibrium prices<sup>24</sup>. The existence of a structured market like the one described above also permits to those interested in analysing the events occurring in the exchange (as in our case) to rely on the availability of data and time series useful to interpret the dynamics underlying the formation of energy prices.

The IPEX includes a spot market (MPE Mercato Elettrico a Pronti) and a future market (MTE Mercato Elettrico a Termine).

The spot market includes: daily exchanged products market (MPEG, Mercato dei Prodotti Giornalieri), day-ahead market (MGP, Mercato del Giorno Prima), Intra-day

---

<sup>20</sup>[www.camera.it/parlam/leggi/deleghe/99079dl.htm](http://www.camera.it/parlam/leggi/deleghe/99079dl.htm)

<sup>21</sup> <https://eur-lex.europa.eu/legal-content/EN/TXT/?uri=CELEX%3A31996L0092>

<sup>22</sup> [https://www.mercatoelettrico.org/It/MenuBiblioteca/Documenti/20200101\\_Vademecum\\_PCE\\_IT.pdf](https://www.mercatoelettrico.org/It/MenuBiblioteca/Documenti/20200101_Vademecum_PCE_IT.pdf)

<sup>23</sup>[https://www.mercatoelettrico.org/It/MenuBiblioteca/Documenti/VademecumBorsaElettricaltaliana\\_def.pdf](https://www.mercatoelettrico.org/It/MenuBiblioteca/Documenti/VademecumBorsaElettricaltaliana_def.pdf)

<sup>24</sup>

[https://www.mercatoelettrico.org/It/MenuBiblioteca/Documenti/MercatiperAmbientedelGME\\_def.pdf](https://www.mercatoelettrico.org/It/MenuBiblioteca/Documenti/MercatiperAmbientedelGME_def.pdf)

market (MI, Mercato Infragiornaliero) and the market for the service of dispatching (MSD Mercato del Servizio di Dispacciamento)<sup>25</sup>. The MGP is the most important exchange where the largest part of the transactions occurs.

### III.2 Time series of the Energy Prices

The time series, composed by the electricity prices of the IPEX on which our analysis has been performed, have been retrieved from the web site of Gestore del Mercato Elettrico (GME). We consider prices from April 2004, that is, from when the exchange initiated its activity, until December 2019. We decided to consider prices until December 2019 in order to avoid including the effects of the pandemic crisis which strongly conditioned consumers' behaviour all over the world with a direct impact on energy price. This impact would be reflected in the trend and volatility of our time series and, given that we do not expect a similar event to repeat within the horizon of our project, we want to exclude this effect from our analysis.

The data available online published by Gestore del Mercato Elettrico are grouped in different Excel spreadsheets, one for each year. Each spreadsheet is composed by 4 tabs: the first one explaining the abbreviations used in the file, the second containing the hourly prices, one with the purchases volume and the last one with the sales volume. We are only interested in the information about prices contained in the second tab: this is organized in such a way that on the first columns days and hours are ordered while on the first row there are the different areas where the IPEX have concurred to the price determination. These areas are: Italy (indicated as "PUN" Prezzo Unico Nazionale – Single National Price), Austria, Brindisi, Calabria, Central-Northern Italy, Corsica AC, Corsica, Central-Southern Italy, Neighbouring Country North-East, Neighbouring Country North-West, Neighbouring Country South, Neighbouring Country Corsica, Foggia, France, Greece, Monfalcone, Northern Italy, Piombino, Priolo G., Rossano, Sardegna, Sicilia, Slovenia, Southern Italy, Switzerland, Turbigio-Ronco.

---

<sup>25</sup> [https://www.mercatoelettrico.org/It/MenuBiblioteca/Documenti/20200101\\_GuidaME.pdf](https://www.mercatoelettrico.org/It/MenuBiblioteca/Documenti/20200101_GuidaME.pdf)

	A	B	C	D	E	F	G	H	I	J	K	L	M	N	O	P	Q	R	S	T	U	V	W
1	Data/Date (YYYYMMDD)	Ora Hour	PUN	AUST	BRNN	CALB	CNOR	CORS	CSUD	E_NE	E_NW	FRAN	GREC	MFTV	NORD	PBNF	PRGP	ROSN	SARD	SICI	SLOV	SUD	SVIZ
2	20040401	1	35.45	35.00	30.25	30.25	35.00	55.00	35.00	35.00	35.00	35.00	30.25	0.00	35.00	35.00	30.25	30.25	55.00	30.25	35.00	35.00	35.00
3	20040401	2	33.06	32.26	30.51	30.51	32.26	55.00	32.26	32.26	32.26	32.26	30.51	0.00	32.26	32.26	30.51	30.51	55.00	30.51	32.26	32.26	32.26
4	20040401	3	32.01	31.09	30.44	30.44	31.09	55.00	31.09	31.09	31.09	31.09	30.44	0.00	31.09	31.09	30.44	30.44	55.00	30.44	31.09	31.09	31.09
5	20040401	4	31.02	30.00	30.00	30.00	30.00	55.00	30.00	30.00	30.00	30.00	30.00	0.00	30.00	30.00	30.00	30.00	55.00	30.00	30.00	30.00	30.00
6	20040401	5	31.22	30.21	30.21	30.21	30.21	55.00	30.21	30.21	30.21	30.21	30.21	0.00	30.21	30.21	30.21	30.21	55.00	30.21	30.21	30.21	30.21
7	20040401	6	30.82	31.76	30.25	30.25	31.76	55.00	31.76	31.76	31.76	31.76	30.25	0.00	31.76	31.76	0.00	30.25	55.00	0.00	31.76	31.76	31.76
8	20040401	7	35.72	35.00	35.00	35.00	35.00	55.00	35.00	35.00	35.00	35.00	35.00	0.00	35.00	35.00	34.56	35.00	55.00	34.56	35.00	35.00	35.00
9	20040401	8	67.71	68.79	68.79	68.79	68.79	68.79	68.79	68.79	68.79	68.79	68.79	0.00	68.79	68.79	48.62	68.79	68.79	48.62	68.79	68.79	68.79
10	20040401	9	70.04	69.50	69.50	69.50	69.50	85.00	69.50	69.50	69.50	69.50	69.50	0.00	69.50	69.50	68.92	69.50	85.00	69.50	69.50	69.50	69.50
11	20040401	10	69.99	69.46	69.46	69.46	69.46	85.00	69.46	69.46	69.46	69.46	69.46	0.00	69.46	69.46	68.91	69.46	85.00	69.46	69.46	69.46	69.46

Figure 3: Extrapolation of the raw data in the table proposed by the GSE where it can be seen the zonal differentiations and the hourly format

From here the first passage was to extrapolate only the columns that indicate time period and the PUN which is the price of interest of our analysis.

GME dataset includes hourly price for each 0:00-23:00 hour interval but in our analysis we follow Castellini et al. (2020) and restrict the observations to the daily interval between 8:00 and 19:00. This is because this time interval is characterized by solar exposition, a crucial input for the production of energy through a photovoltaic system<sup>26</sup>. In Figure 4, we can see the plot of the raw data of the hourly PUN from April 2004 to December 2019.

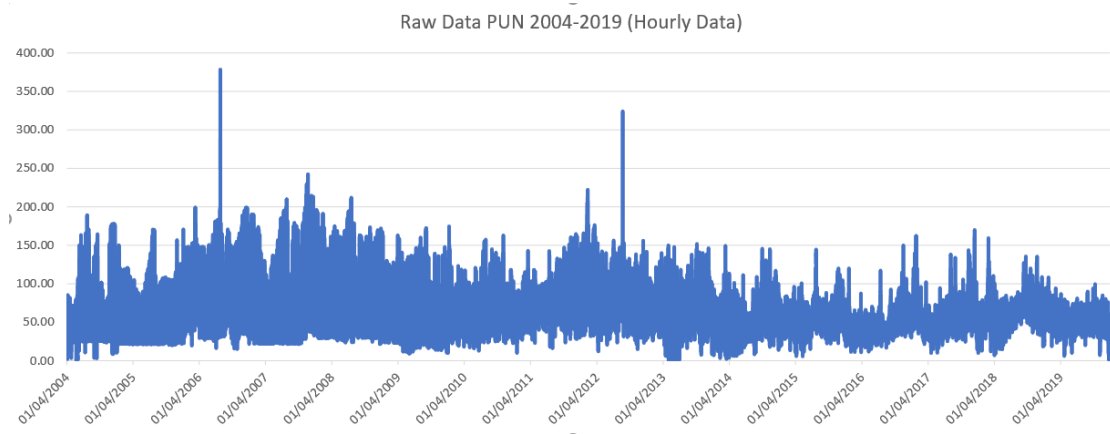


Figure 4: Raw data of the PUN between 2004 and 2019

<sup>26</sup> The data resulting from these elaborations can be seen in Appendix B.1

In Figure 5, we plot the average monthly prices that have been calculated on this new dataset modified as described before. This plot provides a much clearer view of the data than the hourly price in Figure 4.

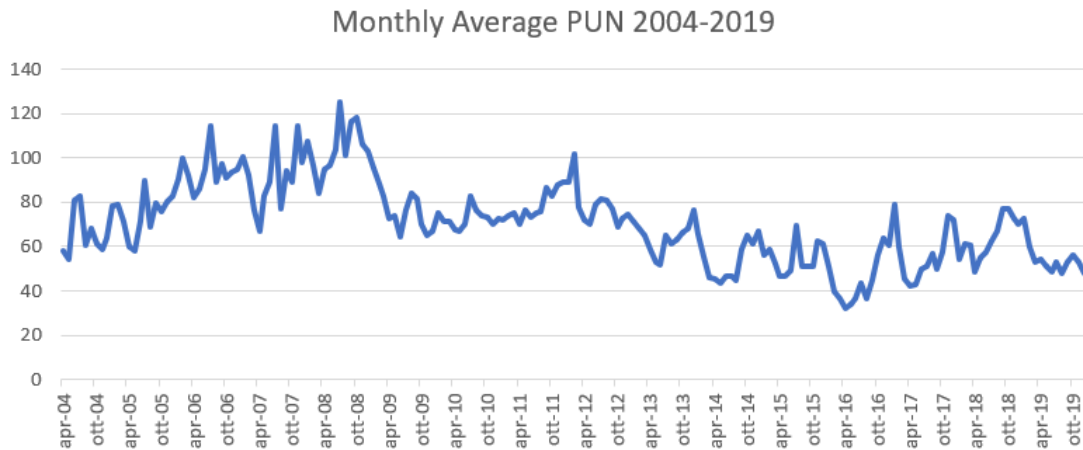


Figure 5: Monthly Average of the PUN between 2004 and 2019

### III.3 Inflation Adjustment

A general decreasing tendency of the energy prices seems to be shown by the data and this trend becomes even more evident once prices are corrected for inflation.

The time series of monthly prices has been adjusted to inflation revaluating each price to its value of December 2019. The inflation rates have been retrieved from inflation.eu in yearly format<sup>27</sup>.

The yearly data have been converted to monthly equivalent through this procedure:

$$i_m = \sqrt[12]{1 + i_y} - 1 \quad (33)$$

$i_m$  = monthly inflation rate       $i_y$  = yearly inflation rate

<sup>27</sup> See Appendix B.2 for the Inflation Rates

An inflation-corrective coefficient equal to 1 (where 1 means no inflation) has been applied to the price of December 2019, that is the date to which all the prices have been actualized. This coefficient has been multiplied by the monthly rate of inflation going backward to the month of November obtaining a compounded rate to be multiplied to the price of the relative month.

The process is repeated until 2004 in order to have an actualization coefficient for each month as can be seen in Figure 6.

Year	Price	Mo Infl	Coef Attu	Actualized Price	Year	Yea Infl
set-18	76.96703	1.00095	1.00940	77.69029	set-18	1.14%
ott-18	77.09695	1.00095	1.00844	77.74795	ott-18	1.14%
nov-18	72.46634	1.00095	1.00749	73.00924	nov-18	1.14%
dic-18	70.17029	1.00095	1.00654	70.62925	dic-18	1.14%
gen-19	72.70013	1.00051	1.00559	73.10655	gen-19	0.61%
feb-19	59.69047	1.00051	1.00508	59.99374	feb-19	0.61%
mar-19	53.13282	1.00051	1.00457	53.37572	mar-19	0.61%
apr-19	54.08659	1.00051	1.00406	54.30632	apr-19	0.61%
mag-19	51.29607	1.00051	1.00355	51.47836	mag-19	0.61%
giu-19	48.66044	1.00051	1.00305	48.80863	giu-19	0.61%
lug-19	53.1677	1.00051	1.00254	53.30260	lug-19	0.61%
ago-19	47.65418	1.00051	1.00203	47.75088	ago-19	0.61%
set-19	53.14555	1.00051	1.00152	53.22641	set-19	0.61%
ott-19	56.26484	1.00051	1.00101	56.32190	ott-19	0.61%
nov-19	53.26682	1.00051	1.00051	53.29382	nov-19	0.61%
dic-19	48.13355		1.00000	48.13355	dic-19	0.61%

Figure 6: partial extrapolation of the process of actualization of the prices

The actualization of the prices has made more evident the overall reduction in the prices over time in real terms respect to nominal terms given the positive inflation occurred in the period considered. In Figure 7, we plot the PUN adjusted for inflation.

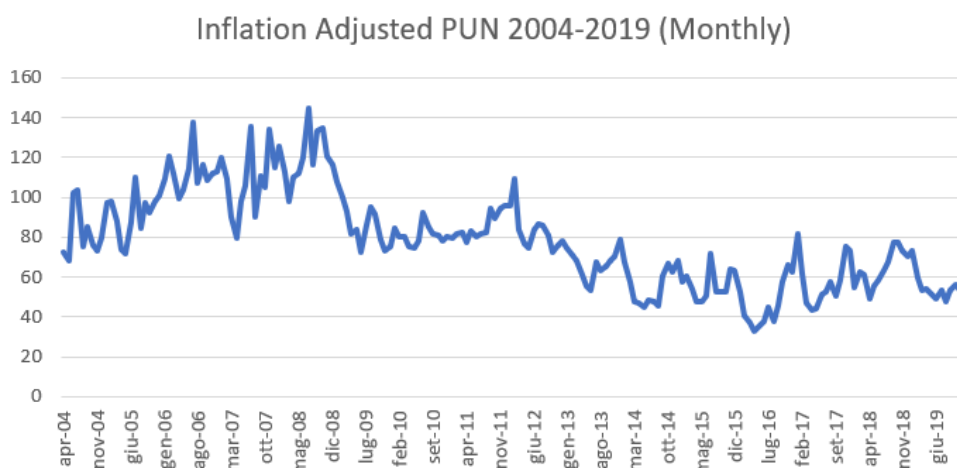


Figure 7: Inflation-Adjusted Monthly Averaged PUN between 2004 and 2019

### III.4 Log Transformation

The data corrected for the inflation in the way described above are then subjected to a logarithmic transformation needed for the next steps of the analysis.

As it was expected, the log transformation reduced the fluctuations of the time series as we can see in Figure 8.

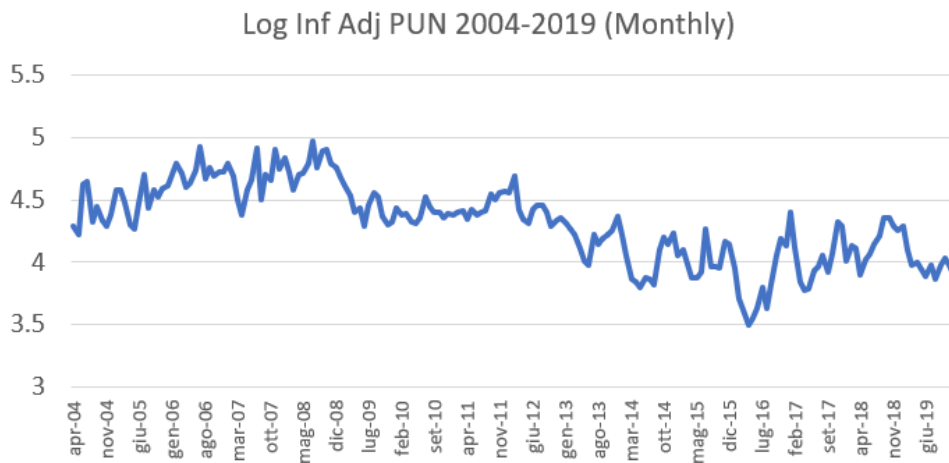


Figure 8: Logarithmic Inflation-Adjusted Monthly PUN between 2004 and 2019

The correlogram of the log-returns in Figure 9 shows a significant autocorrelation only at lag 12 which is a signal of the presence of yearly seasonality in the data as might be expected in a time series of energy prices.

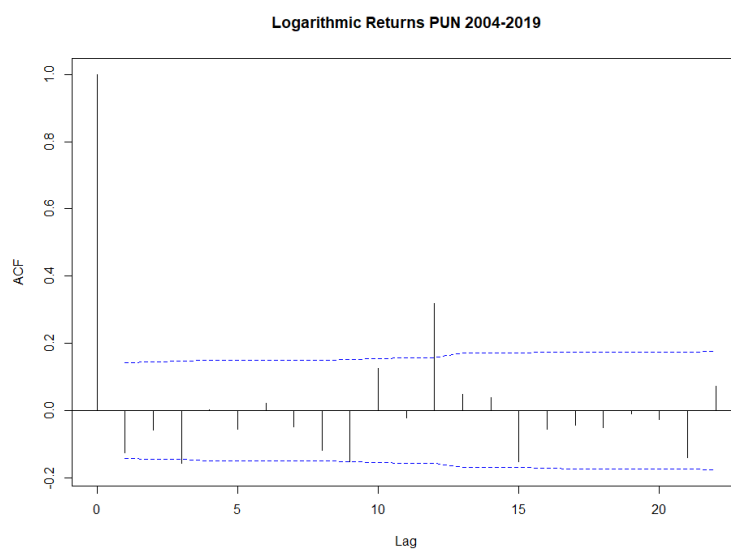


Figure 9: Correlogram of the Logarithmic Returns of the PUN 2004-2019

### III.5 Deseasonalization

Because of the signal in the correlogram, the data has been deseasonalized in order to remove the effect of climate variations during the year that can alter both demand and supply along with other types of cyclical factors.

The process of deseasonalization has been performed using a decomposition with an additive model of the type:

$$Y_t = T_t + S_t + e_t \quad (34)$$

$T = trend$      $S = seasonality$      $e = random\ factor$

Using software R, it has been possible to extrapolate these factors and display them through the function “decompose()” which individuates the trend component through moving average model and excludes it from the time series, after that seasonality is extracted and centred leaving the error term that is determined with the removal of the trend and the seasonal factors from the time series. The use of a moving average model leads to a loss of a starting and an ending part of the time series: in our case the

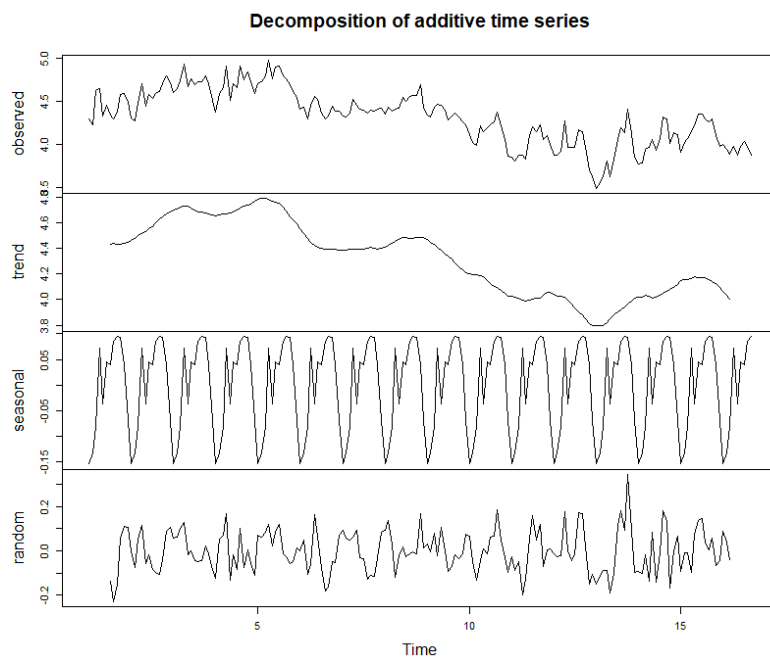


Figure 10: Output of R showing the decomposition of the PUN using the additive method

window of 12 periods for the yearly seasonality involved the loss of the first 6 and the last 6 observations.

The additive model has been preferred to the multiplicative one because through a visual inspection of the plot of the data observed, the magnitude of seasonality does not seem to be proportional to the trend and also because the data were already subjected to a logarithmic transformation. In Figure 11 and 12 the deseasonalized log-data and the log returns are presented.

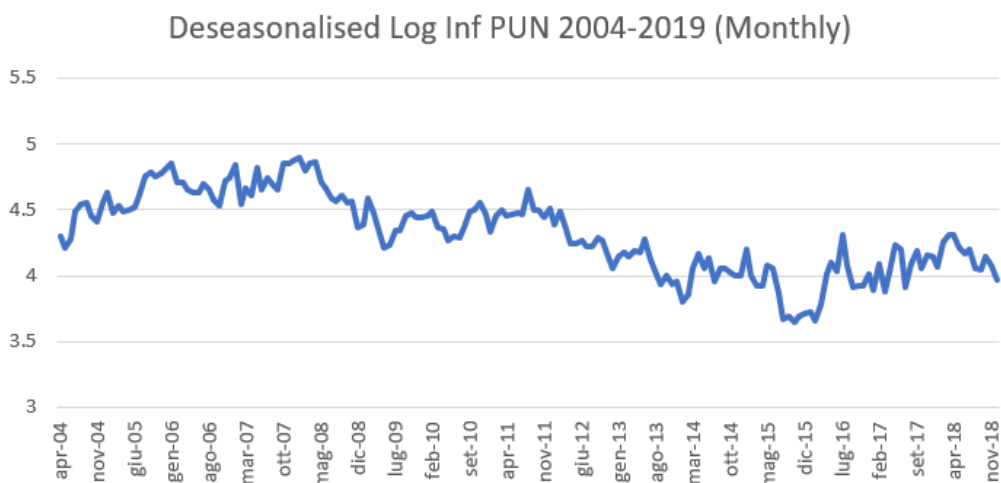


Figure 11: Deseasonalized Logarithmic Inflation-Adjusted PUN 2004-2019

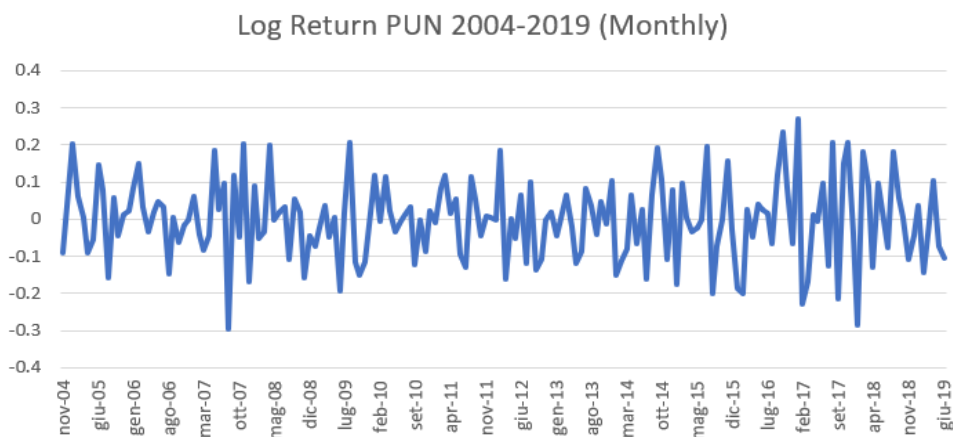


Figure 12: Logarithmic Returns PUN 2004-2019

### III.6 Independence and Normality

The next step was to assess the independence assumption needed to validate the hypothesis by which the PUN can be modelled using a Geometric Brownian Motion.

We notice that the plot of the correlogram in Figure 13 exposes an absence of autocorrelation at all lags. We can compare this correlogram in Figure 13 with the one in Figure 10 to see the effect of the deseasonalization.

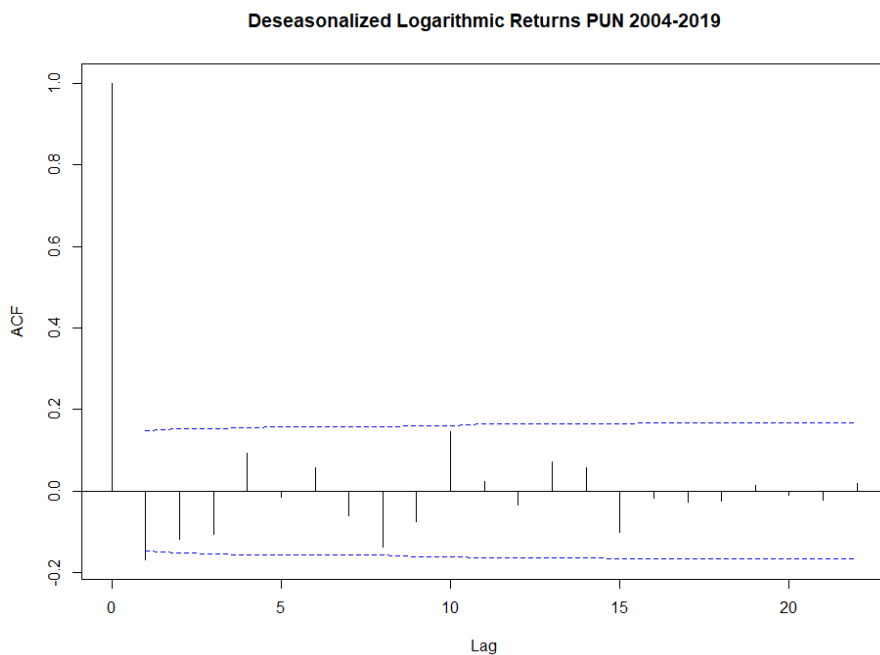


Figure 13: Correlogram of the deseasonalized Logarithmic Returns PUN 2004-2019

With the function “qqplot()” and “qqline()” in software R it has also been possible to visually check for the normality of the data obtaining a superimposition of the sample to the theoretical line representing the normal distribution. The result of this procedure can be seen in Figure 14.

Normality was checked because if we assume that  $p_t$  (PUN) follows a Geometric Brownian Motion then  $\log\left(\frac{p_t}{p_{t-1}}\right)$  should be normally distributed.

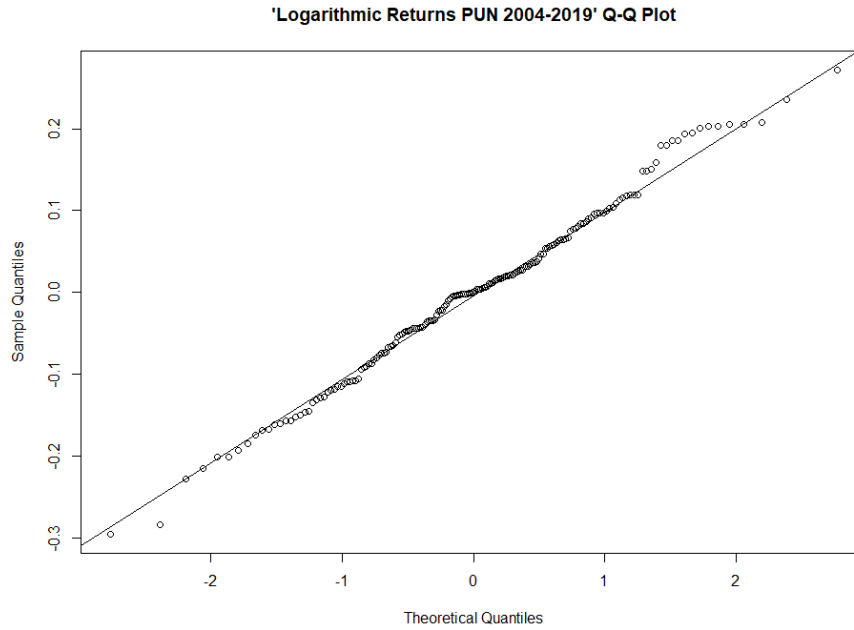


Figure 14: Q-Q Plot of the Logarithmic Returns PUN 2004-2019

### III.7 Non-stationarity

The last step for the validation of the use of the GBM is the test for non-stationarity for which it has been used the Augmented Dickey Fuller ADF test. As it was explained in Chapter 2, this test is structured in such a way that the null hypothesis coincides with the presence of a unit root in the process, that means non stationarity, while the alternative hypothesis suggests stationarity. For our purpose we expect our time series to be non-stationary, so the ADF should not reject the null hypothesis.

The test has been performed using software R through the function `ur.df()` which is composed by different arguments. The first argument requires the specification of the time series that has to be considered. The second is used to specify the type of ADF that has to be performed which can be chosen among “none”, “drift” and “trend”: “none” uses the standard ADF, “drift” corrects in order to account for the presence of a constant drift (that is represented as  $c$  in Equation 35) and “trend” is used to consider both the presence of a constant drift and the presence of a deterministic time trend that can be represented as  $\delta t$  in Equation 36:

$$\text{drift:} \quad y_t = c + \phi y_{t-1} + \epsilon_t \quad (35)$$

$$\text{trend:} \quad y_t = c + \delta t + \phi y_{t-1} + \epsilon_t \quad (36)$$

The argument “lags” specifies the maximum number of lags that have to be included in the formula of the ADF while the argument “selectlags” allows to choose the criteria through which the optimal number of lags has to be selected giving the possibility of using either the Akaike criterion AIC, Bayes criterion BIC or, alternatively, to use exactly the number of lags expressed by the argument “lags” typing “fixed”<sup>28</sup>.

We decided to use the basic model with a maximum number of lags equal to 10 and using the Akaike criterion for the selection of optimal numbers of lags. In figure 15 we can see the output produced by R:

```
> summary(ur.df(n,lags=10,selectlags = "AIC"))
#####
# Augmented Dickey-Fuller Test Unit Root Test #
#####

Test regression none

Call:
lm(formula = z.diff ~ z.lag.1 - 1 + z.diff.lag)

Residuals:
    Min       1Q   Median       3Q      Max
-0.233715 -0.068009 -0.000587  0.063170  0.312381

Coefficients:
              Estimate Std. Error t value Pr(>|t|)
z.lag.1      -0.001219   0.001856  -0.657  0.51219
z.diff.lag1  -0.237230   0.077505  -3.061  0.00258 **
z.diff.lag2  -0.170415   0.078487  -2.171  0.03137 *
z.diff.lag3  -0.153317   0.077092  -1.989  0.04841 *
---
Signif. codes:  0 '***' 0.001 '**' 0.01 '*' 0.05 '.' 0.1 ' ' 1

Residual standard error: 0.1034 on 162 degrees of freedom
Multiple R-squared:  0.07794, Adjusted R-squared:  0.05517
F-statistic: 3.423 on 4 and 162 DF, p-value: 0.01022

value of test-statistic is: -0.6569

Critical values for test statistics:
    1pct   5pct 10pct
tau1 -2.58 -1.95 -1.62
```

Figure 15: Output of R for the Adjusted Dickey Fuller test

<sup>28</sup> <https://www.rdocumentation.org/packages/urca/versions/1.3-0/topics/ur.df>

As we can see in the output presented, the value of the test statistic is -0.6569. We can find in the table in Appendix B.3 the appropriate critical value to which the test statistic has to be compared to assess if the null hypothesis of non-stationarity should be rejected.

We focus on the critical values indicated for model 0, that is the one we used, and check that at this point our sample, after the deseasonalization, contains 177 observations so we consider the row for N=100 (noticing that the difference is not relevant with row N=250 for our comparison). The critical value for level 0.1 is -1.614 which means that our test statistic, equal to -0.6569, suggests that the null hypothesis of non-stationarity cannot be rejected.

### III.8 Parameters Estimation<sup>29</sup>

After having completed the analysis to assess if the PUN time series had the characteristics to be modelled as a Geometric Brownian Motion, we proceed to the estimation of the parameters needed for the model that are drift  $\alpha_P$  and volatility  $\sigma_P$ .

Recall Geometric Brownian Motion equation equal to:

$$dX_t = \alpha_P X_t dt + \sigma_P X_t dW(t) \quad (37)$$

As explained in Chapter 2, by means of Ito's Lemma we know that:

$$y_t = \ln(X_t) \quad dy_t = \left( \alpha_P - \frac{1}{2} \sigma_P^2 \right) dt + \sigma_P dW(t) \quad (38)$$

Given our dataset of log returns, it's useful to express the following discrete time version:

$$y_{t_{n+1}} - y_{t_n} = \left( \alpha_P - \frac{1}{2} \sigma_P^2 \right) (t_{n+1} - t_n) + \sigma_P (W(t+1) - W(t)) \quad (39)$$

---

<sup>29</sup> See Insley (2002) p. 471-492, Bonest and Jun (2006) and Yoshimoto and Kato (2004)

$(y_{t_{n+1}} - y_{t_n})$  follows a normal distribution, because of the properties of the Geometric Brownian Motion, with mean:

$$E(y_{t_{n+1}} - y_{t_n}) = \left( \alpha_P - \frac{1}{2} \sigma_P^2 \right) (t_{n+1} - t_n) \quad (40)$$

and variance:

$$\text{Var}(y_{t_{n+1}} - y_{t_n}) = \sigma_P^2 (t_{n+1} - t_n) \quad (41)$$

It can be noticed that  $t_{n+1} - t_n = 1$ .

Knowing this, it can be proved that the maximum likelihood estimates for  $\alpha_P$  and  $\sigma_P$  parameters of the GBM are:

$$\sigma_P = s \quad (42)$$

$$\alpha_P = m + \frac{1}{2} s^2 \quad (43)$$

where  $s$  refers to the standard deviation of the sample of the log returns that we have analysed and  $m$  refers to the mean of the same sample. The values of  $m$  and  $s$  have been computed with R through the functions `mean()` and `sd()`. They are reported in Table 1 in monthly and annual terms.

MONTHLY		ANNUALISED	
$m$	$s$	$m$	$s$
-0.186%	10.688%	-2.230%	37.025%

Table 1: monthly and annualised estimates for  $m$  and  $s$

Finally, in Table 2 there are the yearly parameters that have been used in our model estimated following the procedure exposed before.

### YEARLY GBM PARAMETERS

$\alpha_p$	$\sigma_p$
4.624%	37.025%

Table 2: estimates for the GBM parameters

### III.9 Final Consumer Price

The price represented by the PUN is the price determined in the IPEX market but it is not equal to the actual price that is paid by a final consumer, mainly because of the costs related to the dispatchment of energy. The analysis performed on the PUN was needed in order to estimate the drift ( $\alpha_p$ ) and the volatility ( $\sigma_p$ ) of the prices of energy given that we assume the PUN as the only stochastic factor in the final consumer price. For this reason, as a matter of tractability, PUN can be considered as a good proxy of the whole price's stochastic characteristics and, therefore, its dynamic has been used to interpret the behaviour of final consumer price in the future.

In the final part of the thesis, we will perform the estimate of the expected time required to reach the Grid Parity. In order to this, we need starting values for both price and cost of energy. Given what we have said before, it would not be correct to use the PUN as starting point for the evaluation in Chapter 5. This is why we refer to the final consumer prices for 2019 published by Autorità per Energia Reti ed Ambiente (ARERA) in order to individuate correctly the starting points to be used in the Grid Parity taking the average of the net prices for the consumption ranges considered<sup>30</sup>. In Table 3 there is an extrapolation of the information in the Appendix with the data on which we are interested divided for residential and commercial consumers.

---

<sup>30</sup> The complete table with the data can be seen in Appendix B.4

		Residential				
Yearly Consumption (KWh)		1.000-2.500	2.500-5.000	5.000-15.000	> 15.000	Average
Net Price (€/kWh)		0.174	0.143	0.127	0.115	0.140

		Commercial					
Yearly Consumption (MWh)		20-500	500-2.000	2.000-20.000	20.000-70.000	70.000-150.000	Average
Net Price (€/kWh)		0.109	0.094	0.090	0.083	0.079	0.091

Table 3: ARERA End Users 2019 Net Prices

As a conclusion of this chapter, in Table 4 we can see all the values estimated in the pages before. These are all the parameters related to price that will be used in the Real Option Grid Parity at the end of the thesis.

	$\alpha_P$	$\sigma_P$	$P_{2019}$
Residential	4.624%	37.025%	0.140
Commercial	4.624%	37.025%	0.091

Table 4: parameters related to price



## IV. Costs

In this chapter we will see how to express the costs related to the PV plant. In the first part, we present the indicators used in the following sections, then we discuss the recent trend of the costs characterising an investment in a PV plant and finally we estimate the parameters of the Geometric Brownian Motion driving, by assumption, the evolution of costs over time.

### IV.1 Measures of Cost

Following the approach of the International Renewable Energy Agency (IRENA), we measure the evolution in time of costs associated to different kinds of sources of energy relying on the following indicators: Total Installed Cost (TIC), the capacity factor and the Levelized Cost of Energy (LCOE). The LCOE is the variable that we are going to use in our analysis together with the PUN, but its estimation depends on the total installed cost and the capacity factor so their comprehension is essential in the general framework.

Generally speaking, the total installed cost is an estimation of the costs associated to the design, the acquisition of the components, the installation and the financing of a fixed asset (which in the case of Solar PV means mainly the module and inverter costs, cabling, grid connection, mechanical and electrical installation, inspection costs, margin of the company apt to the installation for other internal costs). If we consider that construction costs account for the largest part of the whole cost of the PV plant, it is straightforward to understand the close relation between the trend of the TIC and that of the LCOE. This relation is evident by comparing TIC and LCOE in Figure 16. It is also meaningful to underline that construction costs per unit of energy produced have an inverse correlation with the size of the PV plants because of economy of scale: this is the reason why in Figure 18 and Figure 20 we can notice that the costs for the commercial sector are lower than for the residential one.

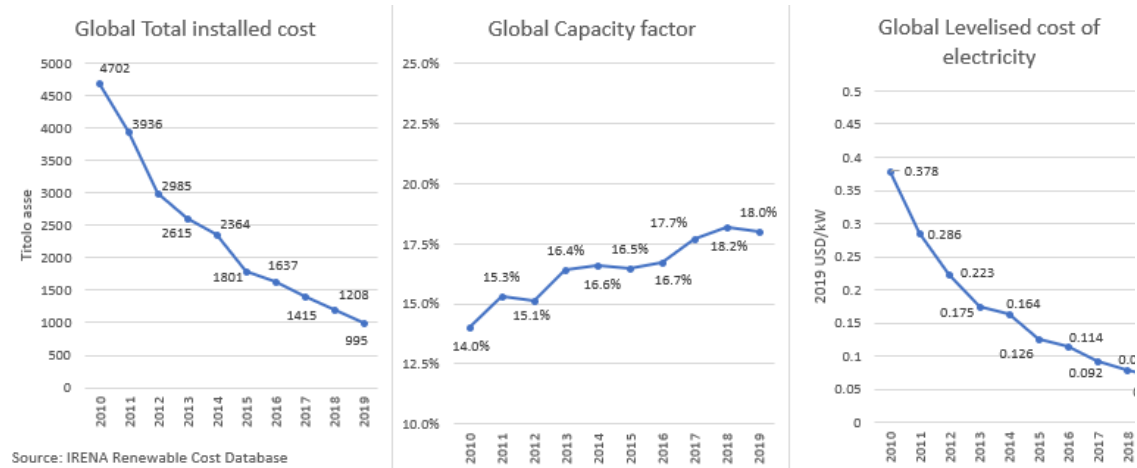


Figure 16: Global Total installed Cost, Capacity Factor and Levelised Cost of Electricity

The capacity factor on the other hand is the percentage that each power generating unit actually produces on average in a period of time respect to the maximum quantity that each unit can produce optimally. Its effect on costs is relevant because a rise in this indicator indicates the possibility of a reduction of the plant's size keeping at the same time the energy output unaltered.

The LCOE is a standard indicator used to compare the cost of electricity produced from different sources of energy and it is the one on which we are going to focus more. It can be defined as the price of electricity in a project satisfying the condition for which revenues equal the present value of all the costs expected in the economic lifetime of the plant, including a return on the capital invested equal to the discount rate.

The LCOEs presented later have been calculated using the following formula:

$$LCOE = \frac{\sum_{t=1}^n \frac{I_t + M_t + F_t}{(1+r)^t}}{\sum_{t=1}^n \frac{E_t}{(1+r)^t}} \quad (44)$$

where:

*LCOE* = the average lifetime levelised cost of electricity generation

*I<sub>t</sub>* = investment expenditures in the year *t*

*M<sub>t</sub>* = operations and maintenance expenditures in the year *t*

*F<sub>t</sub>* = fuel expenditures in the year *t*

$E_t =$  electricity generation in the year  $t$

$r =$  discount rate

$n =$  lifetime of the system

The calculations for the LCOE data used in this paper are based on the total installed cost and the capacity factor plus the Operation and Maintenance expenses which include also insurance and asset management costs.

Difficulties in the estimation of these measures of cost arise from the fast expansion of renewables markets implying an output of renewable energy not always well balanced. This is reflected in an overall volatility of the prices that can increase in period of short-term supply shortage with respect to the demand alternated to periods of supply excess when prices can fall below production costs. This phenomenon makes cost analysis challenging for particular technologies in less stable markets or in periods of great uncertainty.

## IV.2 Global Trend of PV solar energy costs

The costs associated to the production of renewable energy have been subjected to a significant reduction in the past years due to the constant expansion of the relative market and the increase of competition among the producers which led to a consistent improving of the technology involved in the production of these sources of power reaching today a situation in which renewable energy has become a valid cost-efficient choice in the majority of the developed countries<sup>31</sup>. The decrease in the costs have a direct effect on the choices of investment of the energy suppliers: this is supported, for example, by the fact that in 2019 72% of the new electric capacity installed globally was green oriented.

The most interesting aspect of this cost dynamic is the comparison with the fossil fuel-fired alternative: we can see that 56% of the new plants created in 2019 providing energy from renewable sources had lower generation costs than the least expensive carbon-based alternative.

---

<sup>31</sup> See IRENA (2019)

Among the renewable sources of energy, the photovoltaic industry has performed particularly well: in 2019, 40% of the photovoltaic capacity installed costed less than the cheapest fossil fuel-fired project available which is an important goal coming from a long positive trend of the PV sector given that in 2010 the energy from this source was 7.6 times more expensive than the fossil alternative.

At the global level the trend has been consolidating for a decade with the weighted average LCOE of utility photovoltaic systems falling by a dramatic 82% between 2010 and 2019 and by 13% year-on-year only in 2019 hitting 68 USD/MWh at the end of this period. It has been one of the sectors that have experienced the most important cost efficiency improvement in 2010s decade, which is a direct effect of a reduction in the expense associated to PV modules of about 90% in the same period mostly because of their improved performance able to guarantee higher energy output with less surface area. The increasing efficiency of module performance is crucial in the overall cost reduction because reducing the surface needed for one unit of electricity produced has an effect on all the other voices of expenses related to the size of the plant like the racking and mounting structures or cabling.

The global weighted average of total installed cost in 2019 went below the threshold of 1000 \$/kW for the first time reaching 995 \$/kW with a decrease of 79% respect to 2010. This reduction is linked also to the improvement of manufacturing processes along with the development of firms specialized in this field with more experience and better organization in addition to the enhanced module efficiency stated before.

Also, the global weighted-average capacity factor for new utility scale plants was characterised by a positive trend in the decade from 2010 to 2019 starting from 13.8% to 18% at the end of the period. This enhancement in performance measured by the capacity factor was mainly attributed to the expansion of solar energy markets in countries characterised by sunnier weather that have a comparative advantage in the production of solar energy. This kind of weather implies higher irradiation which is the prominent factor in the output per PV module.

### IV.3 Italy's PV solar energy costs data

In Italy, the evolution over time of the PV total installed cost is aligned with the global trend in a very close way as shown by Figure 17.

The weighted average TIC in Italy dropped by 84.3% between 2010 and 2019, a decrease similar to that of the global trend equal to 78.84%, reaching 830 USD/Kw at the end of the period going below the global TIC equal to 995 USD/Kw as we can see in Figure 17. In Figure 18 it is presented the differentiation between total installed costs relative to the residential and the commercial types of PV plants in Italy.

The strong decrease of TIC directly affected the trend of the LCOE. In Figure 19 there's the evidence that the Italian trend is almost identical to the global one, actually the percentage change of weighted average LCOE in the 2010s decade in Italy was equal to -82.12%, very similar to the -82.01% at the global level. In absolute terms, as reported in Table 5, in Italy, the weighted average LCOE reached 0.068 USD/KW coinciding with the global value.

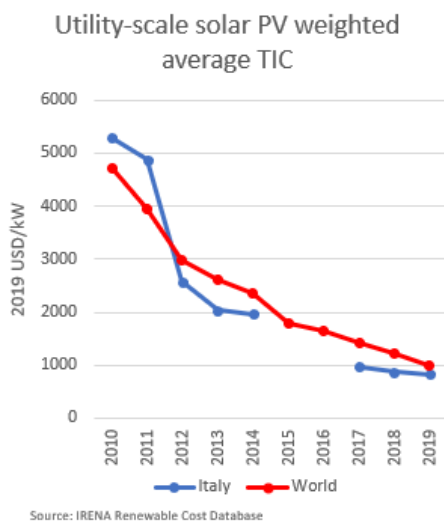


Figure 17: Total Installed Cost comparison between Italy and the World in the period 2010-2019

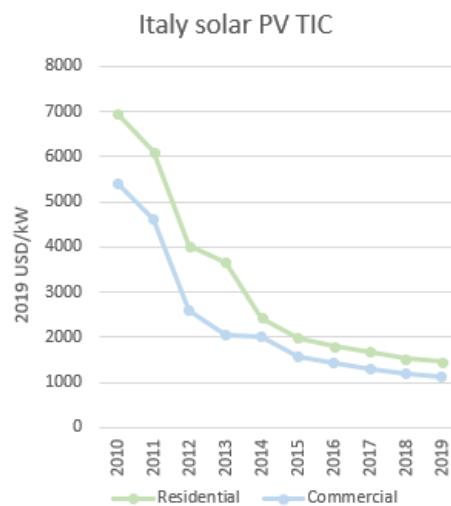


Figure 18: Residential and Commercial Total Installed Cost in Italy

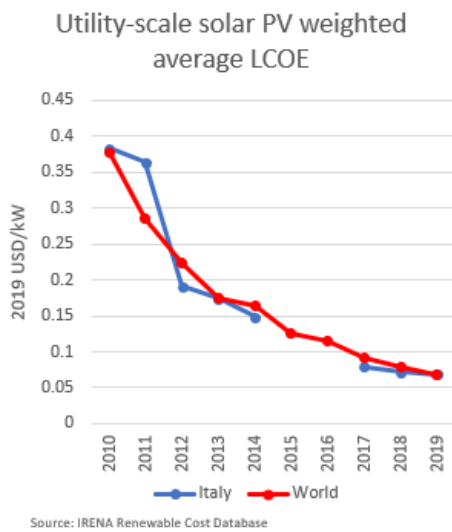


Figure 19: Levelized Cost of Energy comparison between Italy and the World in the period 2010-2019

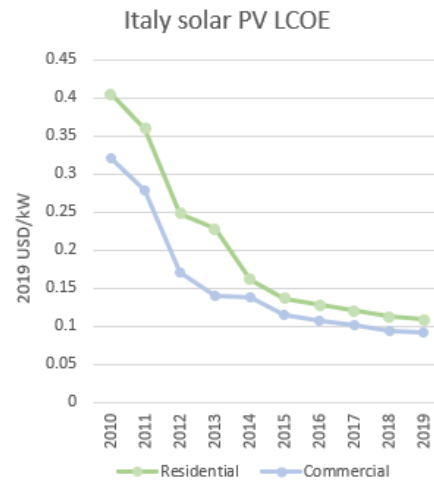


Figure 20: Residential and Commercial Levelized Cost of Energy in Italy

In table 5, we can see the estimates provided by IRENA for the LCOEs between 2010 and 2019 at the global level and in Italy. The Italian data are specified both for the residential and the commercial types of consumers.

Year	World		Italy		
	Utility Scale		Utility Scale	Commercial	Residential
2010	0.378		0.3826	0.322	0.405
2011	0.286		0.3641	0.279	0.36
2012	0.223		0.1906	0.171	0.248
2013	0.175		0.174	0.141	0.228
2014	0.164		0.1482	0.139	0.162
2015	0.126			0.115	0.137
2016	0.114			0.108	0.128
2017	0.092		0.0795	0.101	0.121
2018	0.079		0.0718	0.094	0.113
2019	0.068		0.0684	0.092	0.109
% Change 2010-2019	-82.011%		-82.122%	-71.429%	-73.086%

Table 5: Levelized Cost of Energy comparison in the period 2010-2019

#### IV.4 Learning Curve

For our analysis we used the learning curve method to express the drift of the costs for an estimate of the LCOE in the future. The learning curve methodology is based on the assumption that a market in a phase of development exhibits costs associated to the production characterized by a reduction at a constant rate for each fixed growth of the quantity produced by the industry in that market<sup>32</sup>.

The main economic motivation supporting the choice of this method is that improvements in the production processes occur continuously in the industry of a market that is progressing and enlarging in size. It also considers that in markets that are becoming more mature there are agents that can use their experience and knowledge acquired on the field in order to contribute to improve general efficiency and find solutions to reduce costs. Another advantage of the learning curves methodology is that it is able to embody all this cycle of skills acquisition in one parameter expressing the speed at which the costs aforementioned have been reducing.

Based on these premises we can express LCOE at future time  $t$  as:

$$LCOE_t = LCOE_{2019} e^{\alpha_c \cdot t} \quad (45)$$

where:

$$\alpha_c = LN \cdot GR$$

$$LN = \frac{\ln PR}{\ln 2}$$

$$PR = 1 - LR$$

$GR$  = average growth rate of the industry

$LN$  = learning coefficient

$PR$  = progress rate

$LR$  = learning rate

---

<sup>32</sup> See Nemet (2006)

The learning rate (LR) is generally defined as the percentage fall in costs measured each time the PV solar capacity doubles while the average growth rate in our case is calculated as the yearly percentage change in the PV capacity installed.

According to the International Energy Agency (IEA), the learning rate at the global level since the 1970s to 2020 was equal to 24% even if they underline that taking in consideration a shorter period limited to more recent years may have an important impact on the indicator pushing it above 30%<sup>33</sup>.

Similar results are shown by IRENA: in their report they specify that the learning rate estimated over the period between 2010 and 2019 is equal to 36%<sup>34</sup>.

For the sake of completeness, we have presented the learning rates presented by both the Agencies: the historical rate presented by IEA of 24% has the advantage of a longer time series less subjected to random variations while the rate presented by IRENA of 36% is based on more recent data. Considering that IEA in its report states that a learning rate above 30% would represent better the recent trend, we will stick to IRENA's learning rate equal to 36% for the calculation of our learning coefficient.

On the other hand, for the estimation of the growth factor, according to IEA Italy's PV capacity is expected to expand from 20.9 GW in 2019 to 21.7 GW in 2020 equal to a growth of 3.83% year-on-year. This value is coherent with the growth of the previous years in the Italian market as can be seen in Table 6 reporting the installed capacity between 2013 and 2019 on which the growth factors have been autonomously computed (using GSE data)<sup>35</sup>.

Nonetheless, the Italian National Energy and Climate Plan<sup>36</sup> (prepared by the Italian Government) sets as a long term target a PV installed capacity of 52 GW by 2030 which implies a yearly growth rate of 9% based on a starting point of 20.9 GW in 2019.

We can consider 3% as a conservative GR taken from the IEA approach and a 9% more optimistic GR based on the long run forecasts of the National Energy and Climate Plan.

---

<sup>33</sup> See "Energy Technology Perspectives 2020", IEA (2020), p. 80

<sup>34</sup> See "Renewable Power Generation Costs in 2019", IRENA (2020), p.39

<sup>35</sup> See "Rapporto Statistico 2019", GSE (March 2021), p.44

<sup>36</sup> See "Piano Nazionale Integrato per l'Energia e il Clima (PNIEC)" (2019), p. 58, Table 10

The PNIEC contains the Italian national 2030 targets for energetic efficiency, renewable sources of energy and the reduction of pollution. "Piano Nazionale Integrato per l'Energia e il Clima (PNIEC)", Ministero dello Sviluppo Economico (December 2019)

[https://ec.europa.eu/energy/sites/ener/files/documents/it\\_final\\_necp\\_main\\_it.pdf](https://ec.europa.eu/energy/sites/ener/files/documents/it_final_necp_main_it.pdf)

	Italy Installed PV Capacity (MW)	% YoY Change
2013	18185	
2014	18594	2.25%
2015	18901	1.65%
2016	19283	2.02%
2017	19682	2.07%
2018	20108	2.16%
2019	20865	3.76%

Source: GSE

Table 6: Total Installed Capacity 2013-2019

In Tables 7 and 8 there are the LCOE<sup>37</sup> estimates for 2040 according to the learning curve that we have calibrated divided using the different parameters considered in this chapter, acknowledging that each of their combinations produces a different value of  $\alpha_C$ .

In order to illustrate the evolution of the LCOE in time we also need an estimation of the volatility term to consider possible fluctuations of our forecasts in the future. Defining volatility according to the different types of cost included in the LCOE would be very complicated and misleading, for this reason we decided to focus on the main driver of the LCOE's variations in time, that is, the cost of the PV modules. In this way we are assuming that the volatility related to LCOE can be represented using the volatility of the PV modules cost. As a proxy of this volatility characterizing the modules, we considered some major PV modules producers and used a weighted average of their stocks' prices volatilities that can be easily found given that we are considering listed companies. An estimate of this parameter is provided by Biondi and Moretto (2013) based on the volatility of the four biggest module producers: Yingli Solar, First Solar, Suntech and Trina Solar. On these premises the volatility of the LCOE has been estimated equal to 54%.

---

<sup>37</sup> The LCOE in 2019 are taken from "Renewable Power Generation Costs in 2019", IRENA (2020), p. 73 Table 3.3

## LCOE Forecasts

Conservative GR			
LR <sub>IRENA</sub>			
	Utility	Commercial	Residential
LCOE <sub>2019</sub>	0.068	0.092	0.109
LCOE <sub>2040</sub>	0.046	0.061	0.073

Table 7: Conservative LCOE forecasts

Optimistic GR			
LR <sub>IRENA</sub>			
	Utility	Commercial	Residential
LCOE <sub>2019</sub>	0.068	0.092	0.109
LCOE <sub>2040</sub>	0.020	0.027	0.032

Table 8: Optimistic LCOE forecasts

### IV.5 LCOE's values for the stochastic Grid Parity model

The 2019 LCOEs estimated by IRENA are not readily adapt to be used as inputs in our stochastic Grid Parity model because of 2 reasons:

1. they are expressed in Dollars while the ARERA prices of electricity are expressed in Euros (see Tables 3 and 4)
2. they have been calculated using a discount rate ( $r$  in Equation 44) equal to 5% that is different from the risk adjusted discount rate used in our analysis

In order to produce LCOEs adapt to be compared with the prices in our model we recalculated the LCOEs in IRENA's report using our risk-adjusted discount rate equal to

6.891%<sup>38</sup> and applying the USD/EUR exchange rate on 15/12/2019 equal to 0.899. The LCOEs produced through this method can be seen in the Column “LCOE” in the table below. As a conclusion of this chapter, in Table 9 we can see the parameters related to costs, estimated in the pages before, that will be used in the Real Option Grid Parity in Chapter 5.

	Optimistic Scenario			Conservative Scenario		
	$\alpha_c$	$\sigma_c$	$LCOE_{2019}$	$\alpha_c$	$\sigma_c$	$LCOE_{2019}$
Residential	-5.795%	54.00%	0.117	-1.932%	54.00%	0.117
Commercial	-5.795%	54.00%	0.09	-1.932%	54.00%	0.09

Table 9: parameters related to LCOE

---

<sup>38</sup> The estimation of the risk-adjusted rate is explained in Chapter 5



## V. Grid Parity

The Grid Parity is the first time at which the price of electricity becomes equal to the LCOE associated with PV energy generation. This indicates at which time investing in PV energy generation reaches a break-even point with respect to the alternative, that is, purchasing energy from the National grid. We first determine the Grid Parity under the standard break-even approach and then, using the model provided by Biondi and Moretto (2013), the Grid Parity under a Real Options approach. This is done in order to show the impact of the value of information about future prices and costs on the investment decision. Once presented the models, we use the parameters estimated in the previous Chapters in order to run them in the model and calculate the expected timing of investment.

### V.1 Standard Grid Parity

The solution to the standard Grid Parity problem can be determined by solving the following equation:

$$E_t(P_{t^*}) = E_t(LCOE_{t^*}) \quad (46)$$

where  $E(P_{t^*})$  is the expected value of the price of electricity and  $E(LCOE_{t^*})$  is the expected LCOE at the initial time period  $t=0$  (which coincides with 2019). This equation simply describes the fact that  $t^*$  is the moment at which  $P$  and  $LCOE$  are expected to be equal given the information we have at  $t$ .

$P$  and  $LCOE$  are modelled in the future as GBMs. Here we recall that in Chapter 2 we have seen a useful result that is demonstrated in Appendix A.3, i.e., that the expected value at future time  $t$  of  $X$  modelled as GBM is:

$$E_0(X(t)) = x_0 e^{\alpha t}$$

We can use this result to find  $t$  in Equation 46:

$$E_t(P_{(t^*)}) = P_0 e^{\alpha_P t^*} \quad E_t(LCOE_{(t^*)}) = LCOE_0 e^{\alpha_C t^*}$$

$$P_0 e^{\alpha_P t^*} = LCOE_0 e^{\alpha_C t^*} \rightarrow e^{(\alpha_P - \alpha_C)t^*} = \frac{P_0}{LCOE_0} \rightarrow (\alpha_P - \alpha_C)t^* = \ln \frac{P_0}{LCOE_0}$$

Therefore, the optimal time  $t^*$  at which Equation 46 is satisfied is:

$$t^* = \max\left(\frac{\ln\left(\frac{LCOE_0}{P_0}\right)}{\alpha_p - \alpha_c}, 0\right) \quad (47)$$

where  $\alpha_p$  and  $\alpha_c$  represent the drifts calibrated using the PUN series and the learning curve method while  $LCOE_0$  and  $P_0$  refer to the values of price and cost in 2019 that are set as starting  $t = 0$  ( $P_0 = P_{2019}$  can be seen in Table 4 and  $LCOE_0 = LCOE_{2019}$  can be seen in Table 9).

In our case where  $P_0$  is larger than  $LCOE_0$ , the information provided by the standard Grid Parity is telling us that under a Net Present Value approach the investment should be done as soon as possible: in fact, trying to plug our values in Equation 47, we can see that the time  $t^*$  is negative indicating that the standard Grid Parity has been achieved before time 0 (which coincides with 2019). This means that, according to the standard Grid Parity, the choice to invest is already optimal.

## V.2 Dynamic Programming and Contingent Claim Approaches<sup>39</sup>

Before introducing the stochastic Grid Parity model, in this Section we present the theoretical framework to be used for its set-up.

The problem that we are facing in the analysis conducted in this thesis is particularly complex in its mathematical interpretation because it requires to determine the value of the possibility to invest compared to the possibility to defer the investment not only in the present but at each given time in the future until the decision is made. This means that the problem is composed by a virtually infinite set of possible future choices whose value has to be embodied in the decision to be taken at the evaluation time point. The issue is furtherly complicated by the fact that the expected payoff of this decision depends on two variables that are both stochastic.

The dynamic programming approach is a valid tool for handling this kind of problems. This approach breaks the whole sequence of decisions into just two components: the

---

<sup>39</sup> This Section is based on the Chapters 3-4-5-6 of Dixit Pyndick

immediate decision and a *valuation function* that encapsulates the consequences of all subsequent decisions starting with the position that results from the immediate decision. Basically, if the problem is structured in a finite time horizon, we can determine the payoff of the decision at the last moment available  $T$  and use that as “continuation value” (that means the value of deferring the investment) in the value function at time  $T-1$  (that because if you are in  $T-1$  and decide to defer the investment, you end up by being forced to accept the payoff at  $T$  when the time horizon finishes). In this way it is possible to proceed backward and find the value functions at each time point until the initial one. On the other hand, if the time horizon is infinite (as it is in our case), the problem can be structured in a recursive manner where each decision leads to another problem identical to the previous one.

To illustrate this approach, it may be useful to consider a practical example that can effectively represent the idea of the dynamic programming. Let consider a situation where we must decide whether investing in a project or not. The investment cost is equal to  $I$ . At period 0 the project pays a return equal to  $P_0$  while in period 1 and for the later periods it will produce a return equal to  $(1+u)P_0$  with probability  $q$  and  $(1-d)P_0$  with probability  $(1-q)$ . If we denote by  $V_0$  the value of choosing to invest we have:

$$V_0 = P_0 + [q(1+u)P_0 + (1-q)(1-d)P_0] \left[ \frac{1}{1+r} + \frac{1}{(1+r)^2} + \dots \right]$$

where  $r$  is the discount rate. Note that the first term is the payoff cashed at period 0 while the second represents the expected present value of the future revenue flow.

If the investment decision was available only in period 0, we would have that the payoff  $\Omega$  of the decision at time 0 would be the maximum between the difference  $(V_0 - I)$  and 0:

$$\Omega_0 = \max[V_0 - I, 0]$$

Differently, if we consider the possibility that the investment could be deferred to period 1 with an investment cost still equal to  $I$ , we have a net profit  $F_1$  in period 1 equal to:

$$F_1 = \max[V_1 - I, 0]$$

where  $V_1$  is the expected present value of the revenue flow starting at period 1, that is:

$$V_1 = [P_0(1+u)q + P_0(1-d)(1-q)] \left[ 1 + \frac{1}{1+r} + \frac{1}{(1+r)^2} + \dots \right]$$

Now if we go back to the investment decision to be taken at the beginning of period 0, we have two alternatives: either investing in period 0 cashing ( $V_0 - I$ ) or wait and invest in period 1 obtaining the expected present value  $E_0(F_1)/(1 + r)$ , that is, in algebra:

$$F_0 = \max \left[ V_0 - I, \frac{1}{1 + r} E_0(F_1) \right] \quad (48)$$

In this equation we can see the basic idea of the dynamic programming that is reducing the sequence of decisions to a comparison between the payoff of the immediate choice and the continuation value alternative to the immediate choice which embodies the value of the future decisions. We can notice the difference between  $\Omega_0$  and  $F_0$ : in the first case there is no possibility to defer the investment (a now-or-never decision) while in the second there is the possibility to defer the investment to the next period (with value  $F_1$ ).

We can extend what have been said to cases characterised by more than two periods or where time is continuous.

We define  $\pi_t(x_t, u_t)$  the immediate profit flow depending on the characteristics of the investments described by  $x_t$  (we can imagine  $\pi_t(x_t, u_t)$  as a more general representation of  $V_t - I$  that we have seen before). At time  $t$ ,  $x_t$  is known but the future values  $x_{t+1}, x_{t+2} \dots$  are random variables with a given probability distribution. As a set of random variables ordered in time, they represent a stochastic process. On the other hand,  $u_t$  represents the choices that are available in moment  $t$  that affect the investment (in the simplest case, the one in which we are interested,  $u_t$  can have, for example, value 0 if we choose waiting while having value 1 if we choose investing). Both  $x_t$  and  $u_t$  affect the immediate cash flow  $\pi_t(x_t, u_t)$ . Similar as before, the discount factor between each period is  $\frac{1}{1+r}$  where  $r$  is equal to the discount rate. Furthermore, we define the termination payoff function at time T (when the investment decision ends) as  $\Omega_T(x_T)$ .

With this new set of definitions, we can better define the outcome of the investment, that is, the expected net present value of all the related cash flows  $F_t(x_t)$ . We apply the idea of the dynamic programming that we have expressed before by splitting the investment decision in a choice between the *immediate profit* and the *continuation value* as we did before: in Equation 48 the optimal choice  $u_t$  is *exclusive*, i.e., either

taking the immediate profit flow  $\pi_t$  (that is  $V - I$ ) or the continuation value. But if we want to think about it in a more general way, the choice  $u_t$  may not exclude totally one of the two values, instead it may result in different combinations of the two. The *optimal* choice  $u_t$  is the one producing the better combination.

$F_t(x_t)$  is the sum of the immediate profit and the continuation value when we evaluate them according to the optimal choice  $u_t$ , on which they depend, that maximizes the value of this sum:

$$F_t(x_t) = \max_{u_t} \left[ \pi_t(x_t, u_t) + \frac{1}{1+r} E(F_{t+1}(x_{t+1})) \right] \quad (49)$$

In Eq. 49  $\pi$  is the *immediate profit* while the *continuation value* is the expected value (because  $x_{t+1}$  is a random variable) of the outcome in the next period  $F_{t+1}$  discounted back to  $t$  by the factor  $\frac{1}{1+r}$ .

We can say that Eq. 48 is a special case of the more general Eq. 49 where the choice  $u_t$  imposes to take just one between the immediate profit and the continuation value. For this reason, to replicate the logic of Eq. 48 in the sum of Eq. 49, one of them must take value equal to 0 because of the choice  $u_t$ .

Equation 49 is called the Bellman equation because it is structured according to the basic idea of the dynamic programming and it satisfies the Bellman Principle of Optimality, that is:

*“An optimal policy has the property that, whatever the initial action, the remaining choices constitutes an optimal policy with respect to the subproblem starting at the state that results from the initial action”<sup>40</sup>*

This means that the future choices  $u_{t+1}, u_{t+2}, \dots$  are already considered optimal inside the continuation value and that  $u_t$  is the only choice that has to be made optimally. We can see that the problem has been reduced to a decision in period  $t$ .

To give another form to this equation, we can consider the case in which we have a finite time horizon  $T$  with a *termination payoff*  $\Omega_T(x_T)$  (our *continuation value* in this case).

---

<sup>40</sup> See Dixit and Pyndick pag. 100

It implies that in the period before  $T$  we have  $F_{T-1}$ :

$$F_{T-1}(x_{T-1}) = \max_{u_{T-1}} \left[ \pi(x_{T-1}, u_{T-1}) + \frac{1}{1+\rho} E_{T-1}(\Omega_T(x_T)) \right]$$

From here we can go backwards until the present moment  $t$  knowing that at each step until time  $T$ ,  $u_{t+m}$  is chosen optimally.

In the case of infinite horizon where there is no termination value, the problem is facilitated by the recursive nature of the decision, as we have already said, because at each moment  $t$  we must solve the same optimization problem. This implies that the  $t$  itself has no effect in absolute sense which means that the value function is common to all periods and we can write it without time label, i.e.  $F(x_t)$ . The difference at this point is only in the state variables  $x_t$  where the function  $F(x_t)$  is evaluated in the different periods and the choice  $u_t$ . The Bellman equation becomes:

$$F(x_t) = \max_{u_t} \left[ \pi(x_t, u_t) + \frac{1}{1+r} E[F(x_{t+1})] \right]$$

If we write in general form  $x_t = x$  and  $x_{t+1} = x'$ :

$$F(x) = \max_u \left[ \pi(x, u) + \frac{1}{1+r} E[F(x'|x, u)] \right] \quad (50)$$

This recursive Bellman equation represents a set composed by as many equations as the number of the possible values of  $x$ . The unknowns of these equations are all the values  $F(x)$ . In this sense, Eq. 50 is a functional equation for the unknown  $F$ .

The peculiarity of this functional equation is that we can find the true value function starting with any guess for  $F(x)$ : if we start guessing  $F^{(1)}(x)$ , we proceed by finding the optimal choice  $u^1$  that in turn is substituted back to find  $F^{(2)}(x)$  and repeating the process. This procedure will converge to the true function because of the factor  $\frac{1}{1+r}$  which reduces the error of the guess at each step.

Now if we want to express our problem in continuous time, we can take the limit  $\Delta t$  to 0 and change  $\pi$  so that it expresses the rate of the profit flow and consequently  $\pi \Delta t$  expresses the actual profit flow. The Bellman equation now is:

$$F(x, t) = \max_u \{ \pi(x, u, t) \Delta t + (1 + r \Delta t)^{-1} E[F(x', t + \Delta t) | x, u] \}$$

Now we can multiply by  $(1 + r\Delta t)$ :

$$r\Delta t F(x, t) = \max_u \{ \pi(x, u, t)\Delta t + (1 + r\Delta t)E[F(x', t + \Delta t)|x, u - F(x, t)] \}$$

$$r\Delta t F(x, t) = \max_u \{ \pi(x, u, t)\Delta t + (1 + r\Delta t)E[\Delta F] \}$$

Now divide by  $\Delta t$  and take the limit to 0:

$$rF(x, t) = \max_u \left\{ \pi(x, u, t) + \frac{1}{dt} E[dF] \right\} \quad (51)$$

The left-hand side of this Bellman equation can be seen as the return per unit of time that would be required for holding the asset with a discount rate equal to  $r$  while the right-hand side is composed by immediate payoff  $\pi$  and the expected rate of capital gain.

The case we are facing in this thesis is an optimal stopping problem where we should determine when it is the optimal time to invest in the PV plant and stop waiting. In this situation at each time  $t$  we are facing the decision if to invest and gain  $\Omega(x)$  (the termination payoff that is the payoff from the investment) or to continue waiting and receive the *continuation value* plus the profit flow without investment  $\pi$  (in our case  $\pi = 0$  because there is no profit flow while we wait but we keep it in our notation for generality). In the next moment we face the same choice whose value is embodied in the *continuation value* that we can see as the term on the right inside the following Bellman equation that represents the optimal stopping problem situation:

$$F(x) = \max \left\{ \Omega(x), \pi(x) + \frac{1}{1+r} E[F(x')|x] \right\} \quad (52)$$

One of the key features of a situation of this type is that there will be values larger than  $x^*$  where termination is optimal and values smaller than  $x^*$  where continuation is optimal.

This version of the Bellman equation can be expressed in a more precise way when we consider the case where  $x$  is an Ito Process, that is particularly useful for our aim given that we model the PUN and the LCOE as Geometric Brownian Motions.

So, we have the following increment for  $x$ :

$$dx = a(x, t)dt + b(x, t)dz$$

where  $z$  is a Brownian motion. From the general Bellman Equation for optimal stopping problems in Eq. 52 we have:

$$F(x, t) = \max \left\{ \Omega(x, t), \pi(x, t) + \frac{1}{1+r} E[F(x + dx, t + dt)|x] \right\} \quad (53)$$

where we know that at each moment  $t$  we must decide if stop and get the termination payoff  $\Omega(x, t)$  or continue and get the immediate profit flow  $\pi(x, t)$  plus the value of the choice in the next period (the immediate profit flow  $\pi$  can be 0 if the choice is simply waiting and defer the investment, as it is in our PV plant case, while the termination payoff is the expected present value of the investment minus the cost of the investment). In such a situation, as said before, we have a region upper or lower to  $x^*(t)$  where continuation is optimal and another opposite region where termination is optimal, therefore  $x = x^*(t)$  represents a curve that divides the  $(x, t)$  space into these two regions. Now we suppose that continuation is optimal for  $x > x^*(t)$  (but a similar reasoning can be done for the opposite): in this region we have that the second term of Eq. 53 is larger, therefore because of the max operator:

$$F(x, t) = \pi(x, t) + \frac{1}{1+r} E[F(x + dx, t + dt)|x]$$

We perform the same procedure used for deriving Eq. 51, i.e., multiply by  $1 + r\Delta t$ , then divide by  $\Delta t$  and take limit to 0:

$$rF(x, t) = \pi(x, t) + \frac{1}{dt} E(dF) \quad (54)$$

Here we recall that, because of Ito's Lemma, if  $x$  is an Ito Process, then:

$$E[F(x + dx, t + dt)] = F(x, t) + \left[ F_t dt + aF_x dx + b^2 \frac{1}{2} F_{xx} \right] dt + o(dt)$$

where  $o(dt)$  represents the terms derived from the Ito's Lemma that go to zero faster than  $\Delta t$  which vanish in the limit. This can be used in Eq. 54 in that:

$$E(dF) = E[F(x + dx, t + dt)] - F(x, t)$$

Hence, from Eq. 54 we get (the arguments  $(x,t)$  are omitted):

$$\frac{1}{2}b^2F_{xx} + aF_x + F_t - rF + \pi = 0 \quad (55)$$

We said before that we are considering the case where continuation is optimal for  $x > x^*(t)$  and we used this assumption to select the largest value in the max operator in Eq. 53, i.e., the continuation value. For this reason, the partial differential equation in Eq. 55 holds for  $x > x^*(t)$ .

We can find the necessary boundary conditions of  $F(x, t)$  and  $F'(x, t)$  along  $x = x^*(t)$  (which is the bound of our region). These conditions are necessary to solve the partial differential equation.

We imposed that where  $x < x^*(t)$ , termination is optimal (and on the contrary where  $x > x^*(t)$  waiting is optimal), which means that by continuity where  $x = x^*(t)$  we have:

$$F(x^*(t), t) = \Omega(x^*(t), t) \quad (56)$$

because  $\Omega$  is the termination value obtained where termination is optimal.

Equation 56 is called the *value-matching condition* because it finds a value for the unknown function  $F$  in the termination region.

The other boundary condition is that the two functions  $F(x, t)$  and  $\Omega(x, t)$  should meet tangentially in  $x^*(t)$  which means that their first derivative is equal on the curve  $x = x^*(t)$ :

$$F_x(x^*(t), t) = \Omega_x(x^*(t), t)$$

This is called the *smooth pasting condition*<sup>41</sup>. The key idea behind this condition is that if the two functions do not meet tangentially, then they must meet with a kink which is non-optimal as a behaviour for the value of the function an instant  $\Delta t$  after the meeting point. If the kink was upward-pointing, for  $x$  slightly greater than  $x^*(t)$  within an interval  $dt$ ,  $\Omega$  would be larger than  $F$ , which is contrary to the definition of the curve  $x = x^*(t)$  (that states that  $F(x^*) = \Omega(x^*)$ , i.e., the curve is composed by points of indifference between the termination and the continuation choices). On the other hand, if the kink

---

<sup>41</sup> This condition arises from a rather technical motivation that we do not elaborate too much in detail here, we just go through the general reasons supporting this result keeping in mind that they can be proved more rigorously than what it is done here. See Dixit and Pindyck (1994) p.130 (Appendix C)

was downward-pointing,  $x^*(t)$  could not be a point of indifference because in that case the continuation choice would always prevail: by waiting an instant longer we could choose the side of the kink on the basis of the next step of  $x$  and the expected value (an average) in  $x^*(t)$  for an instant later would be better than the point of the kink itself exactly because of the shape of the kink.

### V.2.1 The Approach applied to our model

The analysis above has pointed out the boundary conditions necessary to solve the partial differential equation resulting from a general Bellman equation for an optimal stopping problem. In order to find the particular Bellman equation fitting our particular case, we now introduce the *contingent claim* approach which can be used to transform our problem into one solvable with the dynamic programming method seen before.

The contingent claim approach is intended to recreate a riskless portfolio formed by the option to invest (we call it  $F(P, C)$ ), whose value represents the value of the possibility to choose to invest, and its underlying  $P$  and  $C$ . To do so we consider some assets (or combination of assets) able to exactly replicate the stochasticity of the cash inflows from the investment (our PUN whose replicating asset here is called  $P$ ) and the outflows (our LCOE whose replicating asset here is called  $C$ ). Both  $P$  and  $C$  dynamics are expressed with GBMs:

$$\frac{dP}{P} = \alpha_P dt + \sigma_P dz_P \quad \frac{dC}{C} = \alpha_C dt + \sigma_C dz_C$$

where:

$$E(dz_P^2) = dt \quad E(dz_C^2) = dt$$

and because we assumed that PUN and LCOE are uncorrelated we have:

$$E(dz_P dz_C) = \rho_{PC} dt = 0$$

Conversely to the dynamic programming approach, here the risk adjusted discount value for the project  $\mu$  is not chosen arbitrarily but it is computed through the well-known Capital Asset Pricing Model:

$$\mu = r_f + B * MRP \tag{57}$$

where  $\mu$  is the rate of return that an investor is expected to receive to own this asset,  $B$  is the “Beta”, that is, the common measure used to express the correlation of the asset with the movement of the market, and MRP is the Market Risk Premium.

The portfolio that we want to create is long on one unit of the option and short on  $m$  units of P and  $n$  unit of C:

$$F(P, C) - mP - nC$$

The differential of this portfolio can be defined using Ito’s Lemma:

$$d(F - mP - nC) = (F_P - m)dP + (F_C - n)dC + \frac{1}{2}(F_{PP}\sigma_P^2P^2 + 2F_{PC}\rho_{PC}\sigma_P\sigma_C + F_{CC}\sigma_C^2C^2)dt$$

Recall that  $\rho_{PC} = 0$ , therefore we can eliminate the term that includes it.

This portfolio is risky only because  $dP$  and  $dC$  are stochastic but if we choose  $m = F_P$  and  $n = F_C$  we can eliminate these terms and obtain a riskless portfolio which increases at each  $dt$  by:

$$\frac{1}{2}(F_{PP}\sigma_P^2P^2 + F_{CC}\sigma_C^2C^2)dt$$

The holder of the portfolio in order to keep the short position must pay to the holder of the long position an amount equal to the difference between the expected return on the assets P and C, call them  $\mu_P$  and  $\mu_C$ , and their capital gain,  $\alpha_P$  and  $\alpha_C$ . If we indicate these differences with  $\delta$  (such that  $\delta_P = \mu_P - \alpha_P$  and  $\delta_C = \mu_C - \alpha_C$ ), the aforementioned payment will be equal to:  $(m\delta_P P + n\delta_C C)$ . Therefore, the dynamics of our portfolio turns out to be:

$$\frac{1}{2}(F_{PP}\sigma_P^2P^2 + F_{CC}\sigma_C^2C^2)dt - (m\delta_P P + n\delta_C C)dt$$

We set this portfolio exactly to be riskless, therefore, if we want to avoid the possibility of arbitrage, we know that its return must be equal to the risk-free rate of return. We express this equality:

$$\frac{1}{2}(F_{PP}\sigma_P^2P^2 + F_{CC}\sigma_C^2C^2)dt - (m\delta_P P + n\delta_C C)dt = r_f(F - mP - nC)dt$$

Now recall that  $m = F_P$  and  $n = F_C$ , divide everything by  $dt$  and rearrange:

$$\frac{1}{2}(F_{PP}\sigma_P^2P^2 + F_{CC}\sigma_C^2C^2) + (r - \delta_P)F_P P + (r - \delta_C)F_C C - rF = 0 \quad (58)$$

This is a partial differential equation for which we must find the adequate boundary conditions as we have explained for Eq. 55 with the dynamic programming approach.

Using the same reasoning that we adopted there, here we state the value of the choice in the region where it is optimal to invest, i.e, our *value-matching* condition:

$$F(P, C) = \frac{P - C}{\mu}$$

given that, once the investment is made, the value of the project is assumed to be:

$$\Omega = \frac{P - C}{\mu}$$

where  $\mu$  is the risk adjusted discount rate estimated with the Capital Asset Pricing Model expressed by Eq. 57.

Considering that both P and C are unitary measure (both PUN and LCOE are expressed for a unit of energy), it is easier to consider our situation with the ratio between P and C, call it  $p = \frac{P}{C}$ , which makes our problem one-dimensional. We can find the boundary conditions where the investment is optimal in term of this ratio rather than in term of the two separate variables, facilitating the path toward an analytical solution. The value of the option becomes:

$$F(P, C) = Cf\left(\frac{P}{C}\right) = Cf(p)$$

considering that:

$$F(P, C) = \frac{P - C}{\mu} - C = \frac{pC - C}{\mu} - C = C\left(\frac{p - 1}{\mu}\right) = Cf(p)$$

Now we can express the partial derivatives present in Eq. 58 in terms of  $f(p)$ :

$$F_p = f'(p) \quad F_C = f(p) - pf'(p) \quad F_{PP} = \frac{f''(p)}{C} \quad F_{CC} = \frac{p^2 f''(p)}{C}$$

and then substituting them in Eq. 58 gives:

$$\frac{1}{2}(\sigma_p^2 + \sigma_C^2)p^2 f''(p) + (\delta_C - \delta_P)pf'(p) - \delta_C f(p) = 0$$

Or alternatively writing  $\delta_C$  and  $\delta_P$  explicitly:

$$\frac{1}{2}(\sigma_p^2 + \sigma_C^2)p^2 f''(p) + (\alpha_P - \alpha_C)pf'(p) - (\mu - \alpha_C)f(p) = 0 \quad (59)$$

Also, the boundary conditions can be rewritten in terms of  $p$  with the *value matching* condition becoming:

$$f(p) = \frac{p - 1}{\mu}$$

and the two *smooth – pasting* conditions becoming:

$$F_P(P, C) = f'(p) = \frac{1}{\mu} \quad F_C(P, C) = f(p) - f'(p) = -\frac{1}{\mu}$$

The result found in Eq. 59 has the form of a homogenous linear equation of the second order whose solution is a linear combination of two solutions linearly independent, that is:

$$f(p) = A_1 p^{\beta_1} + A_2 p^{\beta_2} \quad (60)$$

where  $\beta_1$  and  $\beta_2$  are the positive and negative roots of the following related quadratic equation:

$$\frac{1}{2}(\sigma_P^2 + \sigma_C^2)\beta(\beta - 1) + (\delta_C - \delta_P)\beta - \delta_C = 0 \quad (61)$$

Now we have to consider more carefully the implications of Eq. 60: when  $p$  tends to 0 (more precisely as a consequence of  $P$  going to 0), we want  $f(p)$  to goes to 0 as well because when the price  $P$  of the underlying of the option is very small, the value of the option related to  $P$  should be very near to 0 considering that the probability for the option to be exercised in the future is near 0 too. Contrarily to this reasoning, in Eq. 60 when  $P$  goes to 0 we see that  $A_2 p^{\beta_2}$  goes to infinity because  $\beta_2$  is the negative root of the aforementioned quadratic equation. Therefore, to avoid this behaviour, we must set  $A_2 = 0$ .

We are left with:

$$f(p) = A_1 p^{\beta_1} \quad \rightarrow \quad f'(p) = \beta_1 A_1 p^{\beta_1 - 1}$$

which can be used together with the boundary conditions stated before:

$$\begin{cases} A p^{*\beta} = \frac{p^* - 1}{\mu} \\ \beta A p^{*\beta - 1} = \frac{1}{\mu} \end{cases}$$

$$A = \frac{1}{\beta p^{*\beta - 1} \mu} \rightarrow \frac{p^{*\beta}}{\beta p^{*\beta - 1} \mu} = \frac{p^* - 1}{\mu}$$

With this set of equations, we can find:

$$p^* = \frac{\beta}{(\beta - 1)} \quad (62)$$

where  $\beta$  is the positive root of Eq. 61.

Eq. 62 gives the value of  $p^*$  that is the threshold  $\frac{P^*}{C^*}$  at which investing is preferred to waiting, given that the boundary condition defining  $p^*$  was built exactly as the bound of the region where the Bellman equation is maximized by investing rather than waiting.

### V.3 Real Option Approach

Now that we have gone through the theory behind our model and having specified the value of the threshold which triggers the investment, it is now possible to apply the stochastic model to our data.

The standard Grid Parity model, seen in Section 5.1, evaluates when the unit price of energy produced by a PV plant will be equal to its unit cost, which is a straightforward way to evaluate the investment choice. Nonetheless, it fails in considering that the information acquired in the time passing during the deferral of the investment has a value that is ignored by the model. The involvement in the investment choice analysis of this value is the core of the Real Option approach which gives a mathematical definition of the information value and integrates it in the overall evaluation. Based on these premises, when considering the Grid Parity one must account for the opportunity cost of not deferring the investment in the same way that it is done with the costs associated with the investment, which is exactly what dynamic programming accounts for in the Bellman equation. This approach can be particularly useful for PV systems because they have very high initial costs associated with the construction of the plant which are usually irreversible.

Equation 63 expresses the value of the opportunity to invest as a function of P and LCOE<sup>42</sup>:

$$F(P, LCOE) = E_0[e^{-\mu t^{**}} (P_{t^{**}} - LCOE_{t^{**}})] \quad (63)$$

Where:

$\mu > 0$      *risk adjusted discount rate*

$t^{**}$         *stochastic Grid Parity time*

$E_t(*)$       *expectation operator at time t*

The condition of the stochastic Grid Parity (price = cost + option value) that must hold is:

$$P_{t^{**}} = LCOE_{t^{**}} + F(P_{t^{**}}, LCOE_{t^{**}}) \quad (64)$$

As we have seen in Section 5.2, the threshold at which the investment is triggered is equal to:

$$p^* = \frac{P^{**}}{LCOE^{**}} = \frac{\beta_1}{\beta_1 - 1} \quad (65)$$

Where  $\beta$  is the positive root of Equation 66:

$$\beta = \frac{\frac{1}{2}(\sigma_p^2 + \sigma_c^2) - (\alpha_p - \alpha_c) + \sqrt{\left(\left(\alpha_p - \alpha_c\right) - \frac{1}{2}(\sigma_p^2 + \sigma_c^2)\right)^2 - 2(\sigma_p^2 + \sigma_c^2)(\alpha_c - \mu)}}{\sigma_p^2 + \sigma_c^2} \quad (66)$$

The stochastic Grid Parity time, that is, the time at which the price is expected to equal the LCOE plus the option value, can be expressed considering the probability distribution of  $t^{**}$  as follows:

$$E(t^{**}) = m^{-1} \left[ \ln\left(\frac{\beta_1}{\beta_1 - 1}\right) - \ln\left(\frac{P_0}{LCOE_0}\right) \right] \quad (67)$$

---

<sup>42</sup> The solution of the problem is provided in Appendix C.1

where:

$$m = \sigma_C^2 + (\alpha_P - \alpha_C) - \frac{1}{2}(\sigma_P^2 + \sigma_C^2) \quad (68)$$

The parameters included in Equation 66 are available from the analysis performed in the previous chapters except for the risk adjusted discount rate  $\mu$ .

We estimate this parameter with the classical method of the Capital Asset Pricing Model (CAPM):

$$\mu = r + B(MRP) \quad (69)$$

where

$r$  risk free interest rate

$B$  CAPM Beta measuring the correlation with the systematic risk

$MRP$  Market Risk Premium

The risk-free interest rate has been calculated taking the average of Italian Government Bonds coupon rates between September 2019 and March 2020 with maturities close to 25 years. This calculation gives us a risk free rate of 3.3%<sup>43</sup>.  $B$  has been estimated by Damodaran and it is publicly available in its dataset<sup>44</sup>: the estimate proposed for “Green and Renewable Energy” in Western Europe is equal to 0.57 and it is referred to 05/01/2020. The Market Risk Premium has been taken from Fernandez and al. in their work<sup>45</sup> containing MRP for several countries around the world. The value estimated for Italy in 2019 is equal to 6.3%. Plugging these figures in Equation 54 gives us a risk-adjusted discount rate equal to 6.891%.

In Table 10, we present the stochastic grid parity time calculated plugging into Equation 53 the parameters estimated in the earlier Chapters. In Table 10, we also find the expected time needed in order to reach the stochastic grid parity (expressed in years) considering December 2019 as a starting point and the dates at which the parity is

---

<sup>43</sup> See Bertolini et. al (2018) for a similar procedure

<sup>44</sup> [http://www.stern.nyu.edu/~adamodar/New\\_Home\\_Page/data.html](http://www.stern.nyu.edu/~adamodar/New_Home_Page/data.html)

<sup>45</sup> Fernandez et al., “Market Risk Premium and Risk-Free Rate used for 69 countries in 2019: a survey”, IESE Business School (2019)

expected to be reached. We present our results for both residential and commercial types of investors and according to the scenarios (conservative and optimistic) elaborated on the two Learning Coefficients presented in Chapter 4.

	Optimistic Scenario		Conservative Scenario	
	E(t**) in years	Expected Date	E(t**) in years	Expected Date
Residential	14.2	feb-34	17.3	mar-37
Commercial	15.1	gen-35	18.4	mag-38

Table 10: Expected Time to Threshold and Expected Dates

From the results presented, it follows that including the value of the option to defer the investment in the analysis leads to a significant postponement of the optimal time to invest with respect to the standard Grid Parity approach in Section 5.1 which suggested investing at once. This postponement is due to the uncertainty surrounding the future evolution of the prices of electricity and the costs associated to the investment in a PV plant, that are embodied in the parameters  $\sigma_P$  and  $\sigma_C$ , respectively. This gives value to the opportunity of waiting and acquiring the information provided by the realization of a part of the future paths of prices and costs. For this reason, we can state that the Real Option approach integrates the opportunity cost of investing in a specific moment, giving up the value of subsequent information, in the overall timing decision.

Our findings in Table 10 related to the Optimistic scenario suggests that a residential investor will reach the threshold of the stochastic Grid Parity in 14.2 years while a commercial investor will reach the threshold in 15.1 years which means an expected date equal to February 2034 for the residential case and January 2035 for the commercial one. The difference in the expected dates associated to the two cases is explained by the different starting values  $P_{2019}$  and  $LCOE_{2019}$  used in the model. They are reported in Table 11:  $P$  is larger than  $LCOE$  in both situations but the difference

between them in the residential case is larger than the one in the commercial case. This implies that the residential investor is characterised by a starting situation more favourable to the investment than the commercial investor and the expected dates estimated by the model are conditioned by this fact.

	$P_{2019}$	$LCOE_{2019}$	$P - LCOE$
Residential	0.140	0.117	0.023
Commercial	0.091	0.090	0.001

Table 11: Differences between P and LCOE

Moving to the Conservative scenario in Table 10, we can see that the expected time to the threshold increases by about three years: in the residential case it is equal to 17.3 years while in the commercial case it is equal to 18.4 years corresponding to the expected dates March 2037 for the former and May 2038 for the latter (the difference between the two has the same motivation as in the previous scenario).

The delay existing between the two scenarios is directly related to the lower drift  $\alpha_C$  estimated in the Optimistic case with respect to the conservative one. A lower negative drift implies a faster decrease of the costs compared to a negative drift closer to 0 and with a faster fall of the costs the time required to the parity is shorter, all other things being equal.

To underline the existing relationship between the Optimistic scenario and the Conservative scenario, in Figure 21 we can see a sensitivity analysis with the different expected dates associated to lower levels of  $\alpha_C$ . We can notice that when the decrease in costs associated with the PV plant is expected to be faster (measured by a lower negative  $\alpha_C$ ), the optimal time to invest is nearer in time. The Optimistic scenario corresponds to the points on the two curves where  $\alpha_C = -5.795\%$ , while the Conservative scenario corresponds to the point where  $\alpha_C = -1.932\%$ .

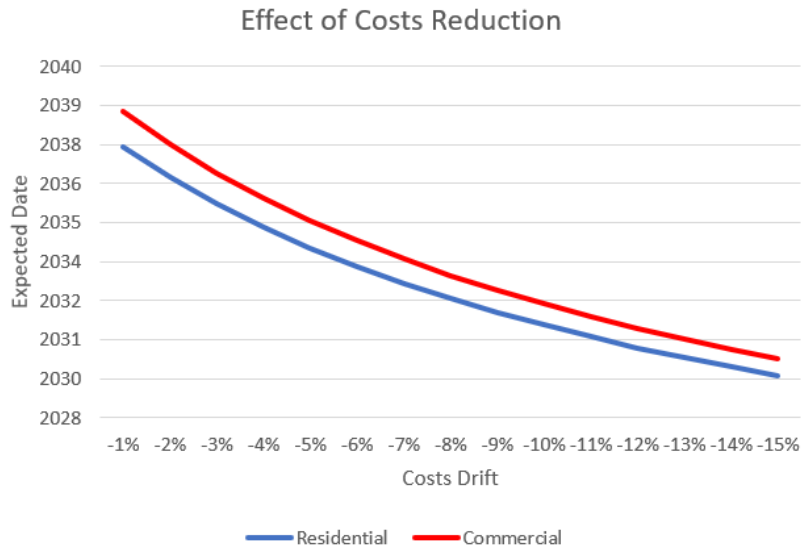


Figure 21: Expected Dates for different levels of the PV plant costs drift

Another important factor affecting the expected time of investment is the risk-adjusted discount rate  $\mu$ . We notice that  $\frac{\partial \beta}{\partial \mu} > 0$ , therefore  $\beta$  is increasing in  $\mu$ . Further, as it can be easily shown  $\frac{\partial E(t)}{\partial \beta} < 0$ , therefore the expected timing of investment is decreasing in the risk-adjusted rate  $\mu$ . In figure 22 we can see the effect of the change in the discount rate on the expected time for the different cases analysed.

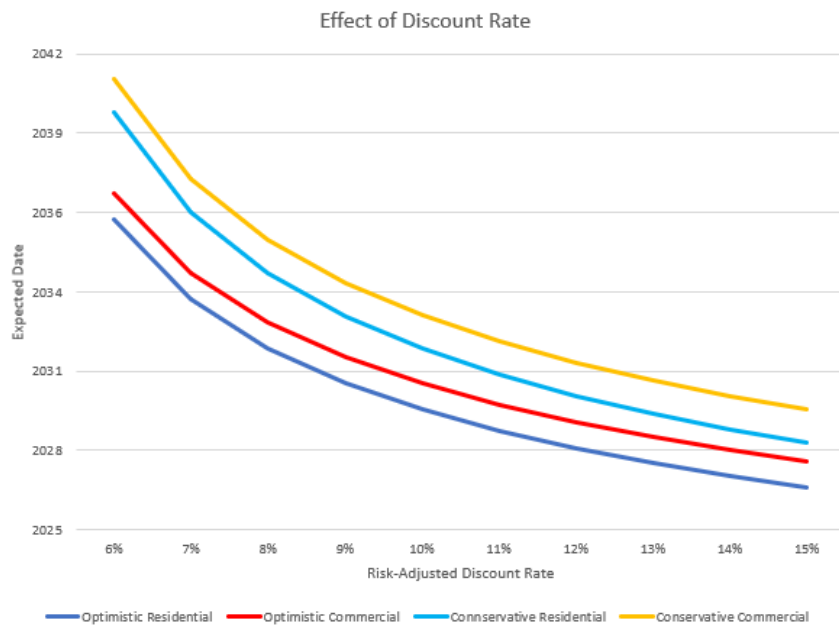


Figure 22: Expected Dates for different levels of the Risk-Adjusted Discount Rate

## VI. Conclusions

In this thesis, starting from an analysis of the Italian energy market, we have seen that the uncertainty characterizing the temporal dynamic of electricity prices and costs associated with PV energy generation affects the decision of an investor about when investment should take place. A standard Grid Parity approach based on a break-even analysis between the energy prices and the Levelized Cost of Energy for the PV sector would suggest that in Italy exists a situation where an investor should invest at once in a PV plant given that the LCOE is lower than the prices of electricity both for commercial and residential consumers.

One of the key points of the thesis is that the standard Grid Parity approach does not adequately represent the timing choice that an investor has to face because it does not consider adequately the irreversibility of the initial investment cost for setting up a PV plant and the uncertain dynamic of electricity prices and generation costs (focusing only on their expected trend).

As shown by Biondi and Moretto (2013), the adoption of a Real Options approach addresses these shortcomings by integrating in the analysis the value of the option to defer the investment and acquiring more information about the evolution of both prices and costs that can relevantly affect the profitability of the project. Using their model, it is possible to determine when the ratio price/costs is expected to reach the threshold level triggering the investment decision.

The results obtained using this model suggest that the uncertainty characterizing electricity prices and the cost of PV energy generation induces a significant delay in the achievement of the parity with respect to the standard approach. We find that the expected time for reaching the Grid Parity varies from 14.2 years for the residential case in the Optimistic scenario to 18.4 years for the commercial case in the Conservative scenario.

In conclusion, the analysis performed in this thesis suggests that there may be still need of some form of incentives supporting the PV energy sector, at least until higher cost-efficiency in the PV energy generation will be reached. The global trend in recent years seems to be favourable toward support by Governments to renewable energy

production and it seems plausible that the achievement of renewable energy generation goals will continue to be a priority for policy makers in Italy and in the world.

## Appendix

### A. Proofs

#### A.1 Variance of the Random Walk

$$\text{Var}(y_t) = E(y_t^2) - E(y_t)^2 = E((y_0 + \sum a_i)(y_0 + \sum a_i)) - y_0^2$$

$$\text{Var}(y_t) = E(y_0^2 + 2y_0\sum a_i + \sum a_i a_j) - y_0^2$$

$$\text{Var}(y_t) = y_0^2 + 2y_0E(\sum a_i) + E(\sum \sum a_i a_j) - y_0^2$$

$$a \sim WN(0, \sigma^2) \rightarrow E(\sum a_i) = 0$$

$$E(a_i a_j) = \begin{cases} E(a_i^2) = \sigma^2 & \text{where } i = j \\ E(a_i^2) = 0 & \text{where } i \neq j \end{cases}$$

$$\text{Var}(y_t) = y_0^2 + 2y_0 * 0 + \sum E(a_i^2) - y_0^2$$

$$\text{Var}(y_t) = \sum_{i=1}^t \sigma^2 = \sigma_{(1)}^2 + \dots + \sigma_{(t)}^2 = t\sigma^2$$

$$\text{Var}(y_t) = \text{Var}(y_0 + \sum a_i) = 0 + \sum \text{Var}(a_i) \quad a_i \perp a_j \text{ if } i \neq j$$

$$\text{Var}(y_t) = \sum_{i=1}^t \text{Var}(a_i) = t\sigma^2$$

Alternatively:

$$\text{Var}(y_t) = \text{Var}(y_0 + \sum a_i) = 0 + \sum \text{Var}(a_i) \quad a_i \perp a_j \text{ if } i \neq j$$

$$\text{Var}(y_t) = \sum_{i=1}^t \text{Var}(a_i) = t\sigma^2$$

A.2 Derivation of the GBM solution formula

From  $BM[W,W](t)=t$  it can be proved that:

$$(dW(t))^2 = dt \quad (dt)(dW(t)) = 0 \quad (dt)^2 = 0 \quad W \sim BM$$

and Taylor's 2<sup>nd</sup> order expansion of a function in  $f$  and  $x$ :

$$\begin{aligned} f(t + dt, x + dx) - f(t, x) \\ \approx f'_t(t, x)dt + f'_x(t, x)dx + \frac{1}{2}f''_{tt}(t, x)(dt)^2 + \frac{1}{2}f''_{xx}(x)(dx)^2 \\ + f''_{tx}(t, x)(dt)(dx) \end{aligned}$$

Given these two premises the Ito-Doebelin formula for an Ito process  $X(t)$ ,  $t \geq 0$  (as defined before) follows (in integral from):

$$\begin{aligned} f(T, X(T)) &= f(0, X(0)) + \int_0^T f'_t(t, X(t))dt + \int_0^T f'_x(t, X(t))dX(t) \\ &\quad + \frac{1}{2} \int_0^T f''_{xx}(t, X(t))d[X, X](t) \\ &= f(0, X(0)) + \int_0^T f'_t(t, X(t))dt + \int_0^T f'_x(t, X(t))\Delta(t)dW(t) \\ &\quad + \int_0^t f'_x(t, X(t))\Theta(t)dt + \frac{1}{2} \int_0^T f''_{xx}(t, X(t))\Delta^2(t)dt \end{aligned}$$

Or alternatively in differential form:

$$\begin{aligned} df(t, X(t)) &= f'_t(t, X(t))dt + f'_x(t, X(t))dX(t) + \frac{1}{2}f''_{xx}(t, X(t))dX(t)dX(t) \\ &= f'_t(t, X(t))dt + f'_x(t, X(t))\Delta(t)dW(t) + f'_x(t, X(t))\Theta(t)dt \\ &\quad + \frac{1}{2}f''_{xx}(t, X(t))\Delta^2 dt \end{aligned}$$

Therefore:

$$\begin{cases} dX(t) = \alpha X(t)dt + \sigma X(t)dW(t) & t \geq 0 \\ X(0) = x_0 \end{cases}$$

$$f(t, X(t)) = \ln X(t) \quad f_t = 0 \quad f_x = \frac{1}{X(t)}$$

$$f_{xx} = \frac{1}{X(t)^2}$$

Because of Ito's Lemma  $d(\ln(X(t)))$  becomes:

$$\begin{aligned} d(\ln X(t)) &= \frac{1}{X(t)} dX(t) + \frac{1}{2} \left( -\frac{1}{X(t)^2} \right) (dX(t))^2 \quad (dX(t))^2 = \sigma^2 X^2 dt \\ &= \frac{1}{X(t)} (\alpha X(t)dt + \sigma X(t)dW(t)) + \frac{1}{2} \left( -\frac{1}{X(t)^2} \right) \sigma^2 X(t)^2 dt \\ &= \left( \alpha - \frac{\sigma^2}{2} \right) dt + \sigma dW(t) \end{aligned}$$

Then we use the integration with the known starting point  $X(0) = x_0$

$$\ln(X(t)) - \ln(X(0)) = \int_0^t \left( \alpha - \frac{\sigma^2}{2} \right) dt + \sigma \int_0^t dW(t)$$

$$\ln\left(\frac{X(t)}{X(0)}\right) = \left( \alpha - \frac{\sigma^2}{2} \right) t + \sigma W(t)$$

$$X(t) = x_0 e^{\left( \alpha - \frac{\sigma^2}{2} \right) t + \sigma W(t)}$$

### A.3 Expected Value of the GBM

$$E(X(t)) = x_0 e^{(\alpha - \frac{\sigma^2}{2})t} \cdot E(e^{\sigma W(t)})$$

The first term on the right is not stochastic, therefore its expected value is simply equal to itself. The stochastic part is the one which comprehends the Brownian Motion  $W(t)$ . We have to compute the expected value of this term  $E(e^{\sigma W(t)})$ .

In order to do this, we have to use the Ito's Lemma and then integrate (recalling that  $W(0) = 0$ ) in a way similar to what have been done in Appendix A.2.

$$E(e^{\sigma W(t)}) :$$

$$d(e^{\sigma W(t)}) = e^{\sigma W(t)} \cdot \sigma dW(t) + \frac{1}{2} e^{\sigma W(t)} \cdot \sigma^2 dt$$

$$f(x) = e^{\sigma x} \quad f'(x) = e^{\sigma x} \cdot \sigma \quad f''(x) = e^{\sigma x} \cdot \sigma^2$$

$$e^{\sigma W(t)} - e^{\sigma W(0)} = \int_0^t e^{\sigma W(s)} \sigma dW(s) + \frac{\sigma^2}{2} \int_0^t e^{\sigma W(s)} ds$$

$$E(e^{\sigma W(t)}) - E(1) = E\left(\int_0^t e^{\sigma W(s)} \sigma dW(s)\right) + \frac{\sigma^2}{2} E\left(\int_0^t e^{\sigma W(s)} ds\right)$$

$$E(e^{\sigma W(t)}) = 1 + 0 + \frac{\sigma^2}{2} \left(\int_0^t E(e^{\sigma W(s)}) ds\right)$$

$$m'(t) = E(e^{\sigma W(t)}) - 1$$

$$m(t) = \int_0^t E(e^{\sigma W(s)}) ds$$

$$\begin{cases} m'(t) = \frac{\sigma^2}{2} m(t) \\ m(0) = 1 \end{cases}$$

$$m(t) = e^{\frac{\sigma^2}{2}t} \cdot m(0)$$

$$E(e^{\sigma W(t)}) = e^{\frac{\sigma^2}{2}t}$$

$$E(X(t)) = x_0 e^{(\alpha - \frac{\sigma^2}{2})t} \cdot e^{\frac{\sigma^2}{2}t} = x_0 e^{\alpha t}$$

#### A.4 Proof of the Martingale Property for the Symmetric Random Walk

In general, a stochastic process  $\{S_t\}$  is a martingale if:

$$E(S_{t+1}|S_t, \dots, S_1) = S_t$$

which means that the expectation of the future conditioned to all past realizations until time period  $t$  depends only on the status of the random variable in time  $t$  without considering what happened before.

For the SRW we consider positive integers  $k < l$  and we define  $F_k$  the information until time  $k$  which mean that  $E(\dots|F_k)$  is the expected value conditioned on the knowledge about what happened until time  $k$ .

$$\begin{aligned} E(M_l|F_k) &= E[(M_l - M_k) + M_k|F_k] \\ &= E[M_l - M_k|F_k] + E[M_k|F_k] \\ &= E[M_l - M_k|F_k] + M_k \\ &= E[M_l - M_k] + M_k = M_k \end{aligned}$$

#### A.5 Proof of the Martingale Property for the Brownian Motion Increments

Given that the Brownian Motion is built on the assumption of the Symmetric Random Walk we can apply the same reasoning.

Consider  $0 \leq s \leq t$  and then:

$$\begin{aligned} E[W(t)|\mathbb{F}(s)] &= E[(W(t) - W(s)) + W(s)|\mathbb{F}(s)] \\ &= E[W(t) - W(s)|\mathbb{F}(s)] + E[W(s)|\mathbb{F}(s)] \\ &= E[W(t) - W(s)] + W(s) \\ &= W(s) \end{aligned}$$

Here we can recall that the conditional expectation of a random variable  $X$  given a  $\sigma$ -algebra  $U$  is itself a random variable identified as  $E(X|U)$ . Loosely speaking, this can be seen as the average of  $X$  over all the possible conditions in  $U$ .

## B. Prices

### B.1 PUN Monthly Average Data<sup>46</sup>

Month	Price	03/2008	84.173942	03/2012	77.983206	03/2016	36.396654
04/2004	57.806392	04/2008	94.714222	04/2012	71.831066	04/2016	31.877726
05/2004	54.145112	05/2008	96.783975	05/2012	69.901533	05/2016	33.912011
06/2004	81.140552	06/2008	104.01636	06/2012	78.716423	06/2016	36.700011
07/2004	82.959628	07/2008	125.51165	07/2012	81.647639	07/2016	43.411951
08/2004	60.445	08/2008	101.37181	08/2012	81.137907	08/2016	36.46365
09/2004	68.345562	09/2008	116.34411	09/2012	77.059359	09/2016	44.481519
10/2004	61.253018	10/2008	118.23606	10/2012	68.999924	10/2016	55.968136
11/2004	58.701434	11/2008	106.10725	11/2012	72.345068	11/2016	63.919549
12/2004	64.014848	12/2008	102.82426	12/2012	74.727494	12/2016	60.493971
01/2005	78.392636	01/2009	95.648658	01/2013	71.41049	01/2017	79.222567
02/2005	79.119089	02/2009	88.781515	02/2013	67.952094	02/2017	59.895209
03/2005	71.46776	03/2009	82.587366	03/2013	65.170327	03/2017	45.438131
04/2005	60.003719	04/2009	72.358014	04/2013	58.643801	04/2017	42.254057
05/2005	58.157239	05/2009	74.234432	05/2013	53.250025	05/2017	42.971585
06/2005	71.115722	06/2009	64.477288	06/2013	51.480065	06/2017	49.898524
07/2005	89.69286	07/2009	76.243777	07/2013	65.329199	07/2017	51.25626
08/2005	68.974671	08/2009	84.290927	08/2013	60.928401	08/2017	56.540054
09/2005	79.462618	09/2009	81.547188	09/2013	63.35864	09/2017	49.520943
10/2005	75.746015	10/2009	69.817485	10/2013	66.119309	10/2017	57.194111
11/2005	80.308708	11/2009	65.247858	11/2013	68.309474	11/2017	73.624004
12/2005	82.971406	12/2009	67.083252	12/2013	76.639222	12/2017	71.807838
01/2006	90.166776	01/2010	75.421	01/2014	65.741652	01/2018	54.000954
02/2006	99.619811	02/2010	71.288433	02/2014	55.802264	02/2018	61.386724
03/2006	92.358021	03/2010	71.6602	03/2014	46.21911	03/2018	60.298105
04/2006	82.048611	04/2010	67.337537	04/2014	45.360599	04/2018	48.711275
05/2006	85.69485	05/2010	66.642102	05/2014	43.318322	05/2018	54.786551
06/2006	94.765338	06/2010	69.980834	06/2014	46.791866	06/2018	57.625665
07/2006	114.53069	07/2010	82.616711	07/2014	46.410429	07/2018	62.244352
08/2006	88.937386	08/2010	76.655405	08/2014	44.461567	08/2018	66.962506
09/2006	97.134579	09/2010	73.693469	09/2014	58.496176	09/2018	76.96703
10/2006	90.963199	10/2010	73.130184	10/2014	64.865241	10/2018	77.096945
11/2006	93.80617	11/2010	70.267476	11/2014	61.010023	11/2018	72.466335
12/2006	94.717017	12/2010	72.787372	12/2014	66.644544	12/2018	70.170291
01/2007	100.82651	01/2011	71.983367	01/2015	55.877862	01/2019	72.700133
02/2007	92.062845	02/2011	74.222641	02/2015	58.439571	02/2019	59.690466
03/2007	76.163577	03/2011	75.114873	03/2015	52.59586	03/2019	53.132821
04/2007	67.037152	04/2011	70.326448	04/2015	46.64586	04/2019	54.086589
05/2007	82.507644	05/2011	76.151925	05/2015	46.600907	05/2019	51.296066
06/2007	89.309604	06/2011	73.179793	06/2015	49.058194	06/2019	48.66044
07/2007	114.80471	07/2011	75.002598	07/2015	69.44892	07/2019	53.167704
08/2007	76.824751	08/2011	75.799307	08/2015	51.016084	08/2019	47.65418
09/2007	93.974596	09/2011	86.892375	09/2015	51.386184	09/2019	53.145551
10/2007	89.162316	10/2011	82.89034	10/2015	50.922888	10/2019	56.264843
11/2007	114.55163	11/2011	87.680491	11/2015	62.466389	11/2019	53.266817
12/2007	97.996638	12/2011	89.143371	12/2015	61.3728	12/2019	48.133553
01/2008	107.22914	01/2012	88.954537	01/2016	50.919933		
02/2008	96.846778	02/2012	101.77965	02/2016	39.486935		

<sup>46</sup> Elaboration of GME data

## B.2 Inflation Rates in Italy<sup>47</sup>

YEAR	INFLATION
2004	2.21%
2005	1.98%
2006	2.09%
2007	1.83%
2008	3.35%
2009	0.78%
2010	1.52%
2011	2.78%
2012	3.04%
2013	1.22%
2014	0.24%
2015	0.04%
2016	-0.09%
2017	1.23%
2018	1.14%
2019	0.61%

## B.3 Augmented Dickey Fuller tables<sup>48</sup>

N	Model 0 - no constant, no trend				Model 1 - constant, no trend				Model 2 - constant, trend			
	0.01	0.025	0.05	0.10	0.01	0.025	0.05	0.10	0.01	0.025	0.05	0.10
25	-2.661	-2.273	-1.955	-1.609	-3.724	-3.318	-2.986	-2.633	-4.375	-3.943	-3.589	-3.238
50	-2.612	-2.246	-1.947	-1.612	-3.568	-3.213	-2.921	-2.599	-4.152	-3.791	-3.495	-3.181
100	-2.588	-2.234	-1.944	-1.614	-3.498	-3.164	-2.891	-2.582	-4.052	-3.722	-3.452	-3.153
250	-2.575	-2.227	-1.942	-1.616	-3.457	-3.136	-2.873	-2.573	-3.995	-3.683	-3.427	-3.137
500	-2.570	-2.224	-1.942	-1.616	-3.443	-3.127	-2.867	-2.570	-3.977	-3.670	-3.419	-3.132
>500	-2.567	-2.223	-1.941	-1.616	-3.434	-3.120	-2.863	-2.568	-3.963	-3.660	-3.413	-3.128

<sup>47</sup> See [www.inflation.eu](http://www.inflation.eu)

<sup>48</sup> <https://www.real-statistics.com/statistics-tables/augmented-dickey-fuller-table/>

B.4 ARERA End User Prices for Energy<sup>49</sup>

RESIDENTIAL cent€/KWh									
Yearly Consumption (kWh)									
< 1.000		1.000-2.500		2.500-5.000		5.000-15.000		> 15.000	
Net	Gross	Net	Gross	Net	Gross	Net	Gross	Net	Gross
32.1	51.19	17.37	24.76	14.3	23.21	12.72	23.07	11.54	22.48

COMMERCIAL cent€/KWh											
Yearly Consumption (MWh)											
< 20		20-500		500-2.000		2.000-20.000		20.000-70.000		70.000-150.000	
Net	Gross	Net	Gross	Net	Gross	Net	Gross	Net	Gross	Net	Gross
18.24	37.48	10.91	22.25	9.41	18.83	8.95	15.81	8.31	12.57	7.85	10.27

<sup>49</sup> Source: “Relazione Annuale Stato dei Servizi, Volume 1”, p. 45 and p. 50, ARERA Autorità Regolazione per Energia Reti e Ambiente

## C. Grid Parity

### C.1 Expected grid parity time<sup>50</sup>

Here we present the solution of the Grid Parity problem under a Real Options approach.

Equation (48) states that:

$$F(P, C) = E_0[e^{-\mu t^{**}} (P_{t^{**}} - C_{t^{**}})]$$

where  $C_t = LCOE_t$ .

According to standard dynamic programming,  $F(P, C)$  is the solution of the following Bellman equation:

$$\mu F(P, C) dt = E_0[dF(P, C)]$$

Applying Ito's Lemma, we can see that  $dF(P, C)$  can be expressed as:

$$\frac{1}{2} (\sigma_P^2 P^2 F_{PP} + \sigma_C^2 C^2 F_{CC}) + P \alpha_P F_P + C \alpha_C F_C - \mu F = 0 \quad (C.1)$$

We can reduce  $F(P, C)$  to one dimension since  $F(P, C)$  is homogenous of degree 1 in  $(P, C)$ . This implies that the optimal choice depends only on the ratio  $p = P/C$ . Hence, we can write:

$$F(P, C) = C f\left(\frac{P}{C}\right) = C f(p)$$

The partial derivatives are as follows:

$$\begin{aligned} F_P &= f'(p) & F_C &= f(p) - f'(p) \\ F_{PP} &= \frac{f''(p)}{C} & F_{PC} &= -\frac{pf''(p)}{C} & F_{CC} &= \frac{p^2 f''(p)}{C} \end{aligned}$$

Equation C.1 can then be rewritten as follows:

$$\frac{1}{2} (\sigma_P^2 + \sigma_C^2) p^2 f''(p) + (\alpha_P - \alpha_C) p f'(p) + (\alpha_C - \mu) f(p) = 0 \quad (C.2)$$

The following boundary conditions must be taken into account:

$$f(p) = p - 1 \quad f'(p) = 1 \quad f(p) - p f'(p) = -1$$

The solution to C.2 takes the following form:

$$f(p) = A p^\beta$$

---

<sup>50</sup> For further details see Biondi and Moretto (2013) "Solar Grid Parity Dynamics in Italy: A Real Option Approach" – Nota di Lavoro FEEM pag. 21-22

where  $\beta (> 1)$  is the positive root of the following equation:

$$\frac{1}{2}(\sigma_P^2 + \sigma_C^2)\beta(\beta - 1) + (\alpha_P - \alpha_C)\beta + (\alpha_C - \mu) = 0$$

that is,

$$\beta = \frac{\frac{1}{2}(\sigma_P^2 + \sigma_C^2) - (\alpha_P - \alpha_C) + \sqrt{\left((\alpha_P - \alpha_C) - \frac{1}{2}(\sigma_P^2 + \sigma_C^2)\right)^2 - 2(\sigma_P^2 + \sigma_C^2)(\alpha_C - \mu)}}{\sigma_P^2 + \sigma_C^2}$$

The optimal threshold to be reached for achieving the Grid Parity is:

$$p^{**} = \frac{P^{**}}{C^{**}} = \frac{\beta}{\beta - 1}$$

The next step is to find the expected time that the process  $p_t$  takes in order to reach  $p^{**}$ . Using Ito's Lemma we can write  $\ln p_t$  as:

$$d \ln p = m dt - \sigma_C dz_C + \sigma_P dz_P$$

where:

$$m = \sigma_C^2 + \alpha_P - \alpha_C - \frac{1}{2}(\sigma_C^2 + \sigma_P^2)$$

The expected time to the threshold is equal to:

$$E(t^{**}) = m^{-1} \left( \ln \left( \frac{\beta}{\beta - 1} \right) - \ln \left( \frac{P_0}{C_0} \right) \right)$$

C.2 Partial Derivative of  $E(t)$  with respect to  $\mu$

We rewrite  $\beta$  as follows:

$$\beta = \frac{C + \sqrt{A + 2B}}{B}$$

where

$$A = \left( (\alpha_P - \alpha_C) - \frac{1}{2}(\sigma_P^2 + \sigma_C^2) \right)^2 - 2(\sigma_P^2 + \sigma_C^2)(\alpha_C)$$

$$B = \sigma_P^2 + \sigma_C^2$$

$$C = \frac{1}{2}(\sigma_P^2 + \sigma_C^2) - (\alpha_P - \alpha_C)$$

Taking the derivative with respect to  $\mu$ :

$$\frac{\partial \beta}{\partial \mu} = \frac{1}{B} \frac{\partial [\sqrt{A + 2B}]}{\partial \mu} = \frac{1}{B} \frac{1}{2\sqrt{A + 2B}} (2B) = \frac{1}{\sqrt{A + 2B}} > 0$$

Taking the derivative of

$$E(t) = \frac{1}{m} \left( \ln \left( \frac{\beta}{\beta - 1} \right) - \ln \left( \frac{P_0}{LCOE_0} \right) \right) = \frac{1}{m} \left( \ln \beta - \ln(\beta - 1) - \ln \left( \frac{P_0}{LCOE_0} \right) \right)$$

with respect to  $\beta$  yields

$$\frac{\partial E}{\partial \beta} = \frac{1}{m} \left( \frac{\partial}{\partial \beta} [\ln \beta] - \frac{\partial}{\partial \beta} [\ln(\beta - 1)] \right) - 0 = \frac{1}{m} \left( \frac{1}{\beta} - \frac{1}{\beta - 1} \right) = \frac{1}{m} \left( -\frac{1}{\beta(\beta - 1)} \right) < 0$$

since  $\beta > 1$  and  $m > 0$ .

## References

- Biondi T. and Moretto M., “Solar Grid Parity dynamics in Italy: A real option approach”, Energy – Elsevier (2013)  
(<http://dx.doi.org/10.1016/j.energy.2014.11.072>)
- Bertolini M., D’Alpaos C., Moretto M., “Do Smart Grids boost investments in domestic PV plants? Evidence from the Italian electricity market”, Energy – Elsevier (2018), (<https://doi.org/10.1016/j.energy.2018.02.038>)
- Cryer J. D. and Chan K. S., “Time Series Analysis. With Applications in R”, Springer (2008)
- Castellini M., Menoncin F., Moretto M., Vergalli S., “Photovoltaic Smart Grids in the prosumers investment decisions: a real option model”, Journal of Economic Dynamics and Control - Elsevier (2020)  
(<https://doi.org/10.1016/j.jedc.2020.103988>)
- Decreto Legislativo 16 marzo 1999, n. 79 "Attuazione della direttiva 96/92/CE recante norme comuni per il mercato interno dell'energia elettrica"  
([www.camera.it/parlam/leggi/deleghe/99079dl.htm](http://www.camera.it/parlam/leggi/deleghe/99079dl.htm))
- Directive 2003/54/EC of the European Parliament and of the Council of 26 June 2003 (<https://eur-lex.europa.eu/legal-content/EN/TXT/?uri=CELEX%3A32003L0054&qid=1620843123560>)
- Directive 96/92/EC of the European Parliament and of the Council of 19 December 1996 (<https://eur-lex.europa.eu/legal-content/EN/TXT/?uri=CELEX%3A31996L0092>)

- Evans L. C., “An Introduction to Stochastic Differential Equations”, Department of Mathematics UC Berkeley (2014)
- Fernandez et al., “Market Risk Premium and Risk-Free Rate used for 69 countries in 2019: a survey”, IESE Business School (2019)
- Gestore dei Servizi Energetici (GSE) "Rapporto Statistico 2011" (May 2012)
- Gestore dei Servizi Energetici (GSE) "Rapporto Statistico 2019" (June 2020)
- Gestore del Mercato Elettrico (GME), “Vademecum della Piattaforma dei Conti Energia a Termine (PCE)”,  
([https://www.mercatoelettrico.org/It/MenuBiblioteca/Documenti/20200101\\_Vademecum\\_PCE\\_IT.pdf](https://www.mercatoelettrico.org/It/MenuBiblioteca/Documenti/20200101_Vademecum_PCE_IT.pdf))
- Gestore del Mercato Elettrico (GME), “Vademecum della Borsa Elettrica Italiana”,  
([https://www.mercatoelettrico.org/It/MenuBiblioteca/Documenti/Vademecum\\_BorsaElettricaltaliana\\_def.pdf](https://www.mercatoelettrico.org/It/MenuBiblioteca/Documenti/Vademecum_BorsaElettricaltaliana_def.pdf))
- Gestore del Mercato Elettrico (GME), “I Mercati per l’Ambiente del GME”,  
([https://www.mercatoelettrico.org/It/MenuBiblioteca/Documenti/MercatiperAmbientedelGME\\_def.pdf](https://www.mercatoelettrico.org/It/MenuBiblioteca/Documenti/MercatiperAmbientedelGME_def.pdf))
- Gestore del Mercato Elettrico (GME), “Indicazione per agevolare l’accesso e la partecipazione al mercato elettrico del GME”  
([https://www.mercatoelettrico.org/It/MenuBiblioteca/Documenti/20200101\\_GuidaME.pdf](https://www.mercatoelettrico.org/It/MenuBiblioteca/Documenti/20200101_GuidaME.pdf))
- Hull J. C., “Options, Futures and Other Derivatives”, Pearson (2015)

- Insley M., “A Real Option Approach to the Valuation of a Forestry Investment”, *Journal of Environmental Economics and Management* 44 (2002)
- International Renewable Energy Agency (IRENA), “Renewable Power Generation costs in 2019”, (2020)
- International Energy Agency (IEA), “Energy Technology Perspectives 2020: Special Report on Clean Energy Innovation”, (July 2020)
- International Energy Agency (IEA), “Solar Energy, Mapping the road ahead”, (2019)
- Le Gall J. F., “Brownian Motion, Martingales and Stochastic Calculus”, Springer (2016)
- Ministero dello Sviluppo Economico (MISE), “Piano Nazionale Integrato per l’Energia e il Clima (PNIEC)”, (December 2019)
- Nemet G., “Beyond the learning curve: factors influencing cost reductions in photovoltaic”, *Energy Policy* (2006)
- Olofsson P. and Andersson M., “Probability, Statistics, and Stochastic Processes”, John Wiley & Sons (2011)
- Phillips P. C. B. and Yu J., "Maximum Likelihood and Gaussian Estimation of Continuous Time Models in Finance", *Research Collection School of Economics - Paper 94* (2006)
- RDocumentation, “Augmented-Dickey-Fuller Unit Root Test”, *urca Package* (<https://www.rdocumentation.org/packages/urca/versions/1.3-0/topics/ur.df>)

- Ruppert D., “Statistics and Data Analysis for Financial Engineering”, Springer (2011)
- Shreve S. E., “Stochastic Calculus for Finance II”, Springer (2004)
- Tsay R. S., “An Introduction to Financial Data with R”, Wiley (2013)
- Yoshimoto A. and Kato T., “Effects of Estimation Length on Parameter Estimates of Geometric Brownian Motion for Log Price Dynamics”, Journal of Forest Research (2004)